TAMPEREEN TEKNILLINEN YLIOPISTO
TAMPERE UNIVERSITY OF TECHNOLOGY

Zahra Ziaei

Vision-based Global Path Planning and Trajectory Generation for Robotic Applications in Hazardous Environments

Julkaisu 1375 • Publication 1375

Tampere 2016

Tampereen teknillinen yliopisto. Julkaisu 1375
Tampere University of Technology. Publication 1375

Zahra Ziaei

Vision-based Global Path Planning and Trajectory Generation for Robotic Applications in Hazardous Environments

Thesis for the degree of Doctor of Science in Technology to be presented with due permission for public examination and criticism in Konetalo Building, Auditorium K1702, at Tampere University of Technology, on the 20th of May 2016, at 12 noon.

Tampereen teknillinen yliopisto - Tampere University of Technology
Tampere 2016

Pre-examiners

Prof. Raul Marin
Dept de Ingeniería y Ciencia de los Computadores
Jaume I University
Castellon, Spain

Dr. Tapio Heikkilä
Principal Scientist, VTT Oy
Docent of Systems Engineering, University of Oulu
Oulu, Finland

Opponents

Dr. Tapio Heikkilä
Principal Scientist, VTT Oy
Docent of Systems Engineering, University of Oulu
Oulu, Finland

Prof. Arto Visala
Department of Electrical Engineering and Automation
Aalto University, ELEC School
Espoo, Finland

Custos

Prof. Jouni Mattila,
Department of Intelligent Hydraulics and Automation
Tampere University of Technology
Tampere, Finland

ISBN 978-952-15-3717-2 (printed)
ISBN 978-952-15-3730-1 (PDF)
ISSN 1459-2045

Abstract

The aim of this study is to find an efficient global path planning algorithm and trajectory generation method using a vision system. Path planning is part of the more generic navigation function of mobile robots that consists of establishing an obstacle-free path, starting from the initial pose to the target pose in the robot workspace.

In this thesis, special emphasis is placed on robotic applications in industrial and scientific infrastructure environments that are hazardous and inaccessible to humans, such as nuclear power plants and ITER[1] and CERN[2] LHC[3] tunnel. Nuclear radiation can cause deadly damage to the human body, but we have to depend on nuclear energy to meet our great demands for energy resources. Therefore, the research and development of automatic transfer robots and manipulations under nuclear environment are regarded as a key technology by many countries in the world. Robotic applications in radiation environments minimize the danger of radiation exposure to humans. However, the robots themselves are also vulnerable to radiation. Mobility and maneuverability in such environments are essential to task success. Therefore, an efficient obstacle-free path and trajectory generation method are necessary for finding a safe path with maximum bounded velocities in radiation environments. High degree of freedom manipulators and maneuverable mobile robots with steerable wheels, such as non-holonomic omni-directional mobile robots make them suitable for inspection and maintenance tasks where the camera is the only source of visual feedback.

In this thesis, a novel vision-based path planning method is presented by utilizing the artificial potential field, the visual servoing concepts and the CAD-based recognition method to deal with the problem of path and trajectory planning. Unlike the majority of conventional trajectory planning methods that consider a robot as only one point, the entire shape of a mobile robot is considered by taking into account all of the robot's desired points to avoid obstacles. The vision-based algorithm generates synchronized trajectories for all of the wheels on omni-directional mobile robot. It provides the robot's kinematic variables to plan maximum allowable velocities so that at least one of the actuators is always working at maximum velocity. The advantage of generated synchronized trajectories is to avoid slippage and misalignment in translation and rotation movement. The proposed method is further developed to propose a new vision-based path coordination method for multiple mobile robots with independently steerable wheels to avoid mutual collisions as well as stationary obstacles. The results of this research have been published to propose a new solution for path and trajectory generation in hazardous and inaccessible to human environments where the one camera is the only source of visual feedback.

[1] International Thermonuclear Experimental Reactor
[2] The European Organization for Nuclear Research
[3] Large Hadron Collider

Preface

The study presented in this dissertation was accomplished in the Department of Intelligent Hydraulics and Automation (IHA) at Tampere University of Technology (TUT) from 2011-2015.

I would like to express my deepest gratitude to my supervisor, Prof. Jouni Mattila for his support, guidance, and invaluable encouragement during my research work. I would also like to thank the Head of IHA, Prof. Kalevi Huhtala, and other professors in the department for creating such an enjoyable academic environment. This thesis was funded by the Academy of Finland and Doctoral Program of Concurrent Mechanical Engineering (DPCME). I gratefully acknowledge the DPCME led by Prof. Erno Keskinen, for the financial support.

I am grateful to the staff of IHA as a whole, particularity Dr. Jarno Uusisalo for his help and support. I also want to thank my colleague and researcher Reza Oftadeh for his cooperation during my research work. I am grateful to my former colleagues from DTP2[4] research group in VTT [5] from 2009-2011. Finally, I would also like to thank Dr. Reza Ghabcheloo and Mohammad M.Aref for their helpful comments and discussions.

I wish to express my sincere gratitude to my beloved husband, Alireza, for his endless love, and my dear son Amir Shahryar. During these years, Alireza, Amir Sharyar and I have shared many sad and happy moments together. None of this work would have been possible without their patience, support, and love. Also I would like to mention my lovely newborn son Amir Mahyar who gave me extra love and energy when I needed it the most. Last, but by no means least, I would like to thank my parents Olya and Mohammad for their unconditional sacrifices and encouragement and my siblings Fatemah and Mehdi for their support.

Zahra Ziaei
Tampere, 2015

[4]Divertor Test Platform 2
[5]Valtion Teknillinen Tutkimuskeskus" (Technical Research Center of Finland)

Contents

Abstract **i**

Preface **iii**

List of Figures **vii**

List of Abbreviations **ix**

List of Publications **xi**

1 Introduction **1**
- 1.1 Objectives of the Thesis . . . 3
- 1.2 Research Method and Restrictions . . . 4
- 1.3 Contribution of the Present Research . . . 6
- 1.4 Author's Contribution to the Publications . . . 7

2 Review of the State-of-the-Art **9**
- 2.1 Computer Vision Applications in Robotics . . . 9
  - 2.1.1 CCD Camera System . . . 10
  - 2.1.2 Vision-based Pose Estimation Methods . . . 11
  - 2.1.3 Vision-based Obstacle Avoidance . . . 14
- 2.2 Vision-based Robot Control . . . 15
  - 2.2.1 Position-based Visual Servoing . . . 17
  - 2.2.2 Image-based Visual Servoing . . . 19
- 2.3 Conventional Path and Trajectory Planning Methods . . . 21
  - 2.3.1 Image-based Path Planning . . . 26
  - 2.3.2 Global Path Planning . . . 26
  - 2.3.3 Robots Trajectory Planning . . . 27
    - 2.3.3.1 Manipulators . . . 28
    - 2.3.3.2 Mobile Robots . . . 29
- 2.4 Summary of the State-of-the-Art . . . 33

3 Summary of Publications **35**
- 3.1 Real-time markerless Augmented Reality for Remote Handling system in Bad Viewing Conditions . . . 35
- 3.2 New Scheme for Image Space Path Planning Incorporating CAD-based Recognition Methods for Visual Servoing . . . 36
- 3.3 Assistive Obstacle-Free Path Planning in the Image Space for Teleoperation Tasks Using Monocular Camera . . . 36

3.4 Global Path Planning with Obstacle Avoidance for Omni-directional Mobile Robots Using Overhead Camera 37
3.5 Vision-based Trajectory Planning for Four Wheel Independently Steered Mobile Robots with Maximum allowable Velocities 38
3.6 Vision-Based Path Coordination for Multiple Mobile Robots with Four Steering Wheels Using an Overhead Camera 39

4 Conclusion **41**

Bibliography **43**

Publications **48**

List of Figures

1.1 Navigation is a challenging task for mobile robots intervention in the hazardous CERN tunnels environment for application such as visual inspection, measurements, and maintenance. 1
1.2 Scheme of the proposed vision-based trajectory generation for mobile robots with steerable wheels through only one camera. 4
1.3 Flowchart of the Path Planning (APF+VS) Subsystem and its related software/hardware define the relationship between the motion of a robot desired points in the image space and corresponding motions in the world coordinates. 5

2.1 Mobile robot navigation is a critical component in creating truly autonomous systems. Computer vision applications plays a major role in developing improved and robust navigation algorithms. 9
2.2 This flowchart shows the main levels of 3D model-based pose estimation approaches. 3D model-based pose estimation can be divided into two different types of methods depending on the image features used to evaluate similarity between the rendered model and the input image. 12
2.3 To estimate the pose of the robot-center coordinates with respect to the fixed camera frame, we employ the created CAD model of the robot's base (Comau Smart) while CAD's center frame coincides with the robot-center coordinates. 13
2.4 Appearance-based object (obstacle) detection using the color cues algorithm. 15
2.5 A general model of visual servoing system which can be used with most Position-based Visual Servoing (PBVS) approaches. This model refers a servoing control since image measurements are used to determine the pose of the target with respect to the camera frame. It is based on camera-in-hand configuration, and the objective of servoing is defined as bringing the camera to a desired position with respect to the target. 17
2.6 Coordinates of the PBVS system including the current camera frame, the desired camera frame, and the reference frame 18
2.7 Path planning for mobile robots in cluttered environments with safety constrains in ITER reactor facilities. Approaches of path planning and trajectory optimization based on geometric constrains were studied and tested in the cluttered ITER scenarios by Vale and Ribeiro (2011) 21
2.8 Basic path planning method by road-map methods. 22
2.9 Exact cell decomposition (left) and approximate cell decomposition (right). . 23
2.10 Total potential fields include negative (attractive) potential fields, while the obstacles are characterized by positive (repulsive) potential fields in desired scale. 23

2.11 Mesh plot of repulsive potential function called FIRAS is used for obstacles which is defined in point (0,0) of desired potential surface, (right). Repulsive barrier function for camera's field of view constraint, (left) 25
2.12 The generated path in [**P**3], guarantees that the robot end-effector remains in the camera's field of view during the operation task. This technique gives the operator a depth cue by visualizing the 6D generated path for the end-effector from initial to desired pose in the image space. 26
2.13 Global path planning versus local path planning for unmanned ground vehicles Giesbrecht (2004). 27
2.14 Generated vision-based individual paths in the image space (left) and the corresponding global path in the world coordinates (right), proposed in [**P**6] for three mobile robots with Four-Wheel Steerable (4WS) while avoiding two types of obstacles including: (1) recognized static obstacles in the image space (two bricks) and (2) image boundaries. 28
2.15 Car-like vehicle (a), three-wheeled differential drive (b), and Omni-directional mobile robot (c). 29
2.16 Non-holonomic omni-directional mobile robot with four independently steering wheels, called iMoro Oftadeh et al. (2013a). 30
2.17 Generated synchronized trajectories via vision-based method presented in [**P**5], for the all steering wheels $Q_0, Q_1, ..., Q_4$, simplify the complexity of kinematic model. To plan the robot velocity, the instantaneous center of rotation (ICR) can be estimated using at least two synchronized generated trajectories of the wheels on omni-directional mobile robot. 32

List of Abbreviations

2D	Two-dimensional
3D	Three-dimensional
4WS	Four-Wheel Steerable
6D	Six-dimensional
AR	Augmented Reality
APF	Artificial Potential Field
CAD	Computer-Aided-Design
CCD	Charge Coupled Device
CERN	European Council for Nuclear Research
CMM	Cassette Multifunctional Mover
DOF	Degrees Of Freedom
FIARS	Force Inducing an Artificial Repulsion from the Surface of the obstacle
HSI	Hue, Saturation, Intensity
HSV	Hue, Saturation, Value
ITER	International Thermonuclear Experimental Reactors
IBVS	Image-based Visual Servoing
ICR	Instantaneous Center of Rotation
PBVS	Position-based Visual Servoing
POSIT	Pose from Orthography and Scaling with ITeration
RANSAC	RANdom SAmple Consensus
RH	Remote Handling
RGB	Red, Green, Blue
VS	Visual Servoing
VVS	Virtual Visual Servoing
WHMAN	Water Hydraulic Manipulator

List of Publications

This thesis consists of the following publications. In the text, these publications are referred to as [**P1**],...,[**P6**].

P1 Z. Ziaei, A. Hahto, J. Mattila, M. Siuko, and L. Semeraro, "Real-time markerless Augmented Reality for Remote Handling system in bad viewing conditions," *Fusion Engineering and Design (Elsevier)*, Jan. 2011, vol 86, no. 9, pp. 2033-2038.

P2 Z. Ziaei, R. Oftadeh, and J. Mattila, "New Scheme for Image Space Path Planning Incorporating CAD-Based Recognition Methods for Visual Servoing," in *Proceeding of the IEEE International Conference on Robotics, Automation and Mechatronics*, 2013 (RAM 2013), Manila, Philippines, November 12-14, 2013, pp. 212-217.

P3 Z. Ziaei, R. Oftadeh, and J. Mattila, "Assistive Obstacle-Free Path Planning in the Image Space for Teleoperation Tasks Using Monocular Camera," in *Proceeding of the IEEE International Conference on System Theory, Control and Computing*, 2014 (ICSTCC 2014), Sinaia, Romania, October 17-19, 2014, pp. 838-844.

P4 Z. Ziaei, R. Oftadeh, and J. Mattila, "Global Path Planning with Obstacle Avoidance for Omnidirectional Mobile Robots Using Overhead Camera," in *Proceeding of the IEEE International Conference on Mechatronics and Automation*, 2014 (ICMA 2014), Tianjin, China, August 2-5, 2014, pp. 697-704.

P5 Z. Ziaei, R. Oftadeh, and J. Mattila, "Vision-Based Trajectories Planning for Four Wheels Independently Steered Mobile Robots with Maximum Allowable Velocities," in *Proceeding of the 16th Annual Conference on Towards Autonomous Robotic System*, 2015 (TAROS 2015), Liverpool, England, September 8-10, 2015, Springer, Vol. 9287, pp. 303-309.

P6 Z. Ziaei, R. Oftadeh, and J. Mattila, "Vision-Based Path Coordination for Multiple Mobile Robots with Four Steering Wheels Using an Overhead Camera," in *IEEE International Conference On Advanced Intelligent Mechatronics* , 2015 (AIM 2015), Busan, Korea, July 7-11, 2015, pp. 261-268.

1 Introduction

Robotic and autonomous systems play increasingly important role in industrial and scientific infrastructure environments, such as International Thermonuclear Experimental Reactors (ITER) and European Council for Nuclear Research (CERN) tunnel to enhance maintenance and inspection, see Figure 1.1. The intricacy of such tasks in radioactive environments often mandates the use of high degree of freedom manipulators and dexterous mobile robots with high mobility and maneuverability.

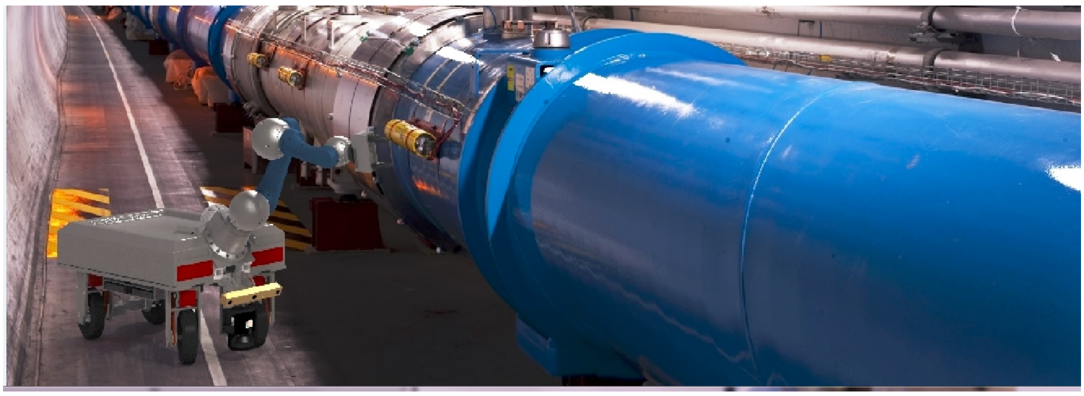

Figure 1.1: Navigation is a challenging task for mobile robots intervention in the hazardous CERN tunnels environment for application such as visual inspection, measurements, and maintenance.

Major areas of research in robotics with a large number of different techniques focus on improving the degree of system autonomy and developing robotic technologies for implementation in variety of industrial applications. Robots are essentially machines that have the power to sense and act based on how they are programmed. Autonomy is an important factor determining the effectiveness of the human-robot system that has been largely explained as an allocation of function between a human and a robot. Robot autonomy refers to the robot's capability to carry out its own processes and operation.

Levels of robot autonomy, ranging from teleoperation to fully autonomous robots, influence the interaction between humans and robots. The benefits of full autonomy can be realized while a robot be able to operate independently of constant human supervision. However, determining appropriate autonomy in a robot is not an exact science. Higher robot autonomy requires less human-robot interaction Yanco and Drury (2004). Recently, Beer et al. (2014) proposed a process for determining a robot's autonomy level from low to high for each of the robot's sense and act by categorizing autonomy along a their defined 10-point taxonomy.

To increase the level of robot autonomy various methods have been proposed during the last few decades. Chintamani et al. (2010) proposed a vision-based method using Augmented Reality (AR) for indoor navigation to reduce the display-control misalignment problem in a teleoperation tasks. Reducing the display control misalignment using AR increases the autonomy of system and produces efficient end-effector navigation in robot workspace. This system automatically recognizes a location by employing a vision system and uses AR to overlay the user's view with location information.

The path planning algorithm proposed by Colito (2007) provides the decision making or logic required for increasing the level of robot autonomy. The path planner must have accurate information about the robot's surrounding environment to make suitable decisions. Vision-based sensors can be included to further improve the robot's environment data. The basic feature of an autonomous mobile robot is its capability to operate the desired task independently in unknown or partially known environments Velagic et al. (2006). The autonomy implies that the robot is capable of reacting to static and dynamic obstacles and uncertain dynamic events in robot workspace. To achieve this level of autonomy, methods need to be developed to provide solutions for navigation, map building, path planning and control. The development of such methods for autonomous robot navigation is one of the main trends in robotics research. Navigation and remote control are major issues in successful operation, inspection, and maintenance applications. Path planning process is the major navigational scheme that increases robot's level of autonomy to plan a safe obstacle-free route through its environment. Based on the information available in the robot workspace, the two main types of path planning methods are global path planning and local path planning.

The main focus in this thesis is on global path planning. Global path planning is a fundamental problem and a key component in creating autonomy for robots. This method usually involves strategies that generate an obstacle-free path based on a pre-known environmental map. Path planning research for autonomous mobile robots has attracted attention since the 1970s. Various path planning methods for obstacle free path planning problem in static environments have been presented in the literature. Ismail et al. (2008) presented genetic algorithm. Kala et al. (2011) proposed a hierarchical solution to this problem using multi-neuron heuristic search. Kuffner and LaValle (2000) proposed a randomized approach to single-query path planning problems in an high-dimensional configuration spaces. The artificial potential field method is normally used for path planning and obstacle avoidance in a static environment. The proposed method by Warren (1989) using Artificial Potential Field (APF) describes a path planning technique for robotic manipulators and mobile robots in the presence of stationary obstacles. This method can be used to solve path planning problems with geometrically different obstacles and offers a fast and effective solution to global path planning problems.

Trajectory planning is to design the configuration of the mobile robot motion as a function of time. Trajectory planning for omni-directional mobile robot is not as well researched as that of mobile robot path planning. This problem consists of three main parts including path planning, translation velocity planning and rotation planning. Omni-directional mobile robots are much more flexible than ordinary non-omni-directional mobile robot, which makes them especially suitable for working in tight space. Wang and Qi (2001) presented a trajectory planning method based on kinematic model for 4WS vehicle in static environments which consists of two parts including rotation planning and translation planning. In this method, the heading angle of the vehicle is required to fully determine the orientation of the robot. The velocity profile is designed so that the vehicle can move at the maximum allowable speed. By utilizing Bezier Curve, trigonometric function and polynomial, a posture planning algorithm for omni-directional mobile robot in static environments is designed by Chen et al. (2012). This method consists of three parts including path planning, line velocity planning and posture planning. However, the major drawback of these methods is their relative complexity in the kinematic and dynamic models.

The most distinguishing aspect of multiple mobile robots compared to a single mobile robot is the possibility of mutual collision. Computation of the intersection region between mutual mobile robots and their swept volume, which determines the geometrical intersection boundaries to avoid mutual collision, is a key solution. Multiple robots path coordination algorithms can be divided into centralized algorithm proposed by Sanchez and Latombe (2002), and decentralized algorithm proposed by Lumelsky and Harinarayan (1997). A centralized planner computes a path and motion in a combined configuration space, which consider the robots as a single combined robot, necessarily. In a decoupled approach, separate paths for each robot are computed independently, and then a coordination diagram plans mutual collision-free trajectory for each robot along its path.

Several path coordination methods have been proposed for multiple mobile robots in a shared workspace. Beard and McLain (2003) presented a method which use a team of robots to cooperatively search an area of interest that contains regions of opportunity and regions of potential hazard. To this end, the robots are constrained to stay within communication range of one another robot. Parker (2009) addressed the problem of path coordination for a team of autonomous mobile robots to share the same workspace while avoiding interference with each other, and/or while achieving group motion objectives. A geometry-based approach for multiple mobile robots motion coordination was proposed by Siméon et al. (2002) to coordinate the motions of several robots moving along fixed independent paths to avoid mutual collisions. The proposed algorithm is based on a bounding box representation of the obstacles in the coordination diagram. Liu et al. (2011) proposed a method for coordination of multiple mobile robots to fulfill formation requirement in moving along specified paths while meeting velocity/acceleration constraints and avoiding collisions.

1.1 Objectives of the Thesis

A critical task in achieving robot autonomy is automatic path planning between the current state and the objective state in a robot workspace. Therefore, the major objectives of this thesis are summarized as follows:

- Provide a markerless AR method to increase the level of autonomy of teleoperation tasks by determining the Six-dimensional (6D) pose of the manipulator's end effector during Remote Handling (RH) tasks.
- Provide a vision-based path planning method to determine the 6D path of the end-effector from initial to desired pose while the camera is mounted on the 6 Degrees Of Freedom (DOF) manipulator's end effector.
- Determine and display the desired 6D path of the end-effector in RH tasks to increase the depth cue for the teleoperator and increase the system performance while the overhead camera is fixed above the manipulator's workspace.

- Provide a new vision-based global path planning method for mobile robots with steerable wheels while avoiding two types of obstacles, including a static object in the image space and image boundaries that act as obstacles and keep the path in the camera's field of view.

- Generate synchronized trajectories for non-holonomic omni-directional mobile robots with steerable wheels to simplify their kinematic models for planning maximum allowable steering and driving velocities.

- Provide a vision-based method for decoupled path coordination of multiple mobile robots with 4WS in shared and confined workspace while keeping within the camera's field of view and avoiding mutual collisions as well as stationary obstacles.

1.2 Research Method and Restrictions

Robotic path planning is a broad field with various potential approaches. The emphasis of this study is on path planning and trajectory generation for non-holonomic mobile robots with 4WS and manipulators with high degree of freedom that are able to follow a 6D generated path. As illustrated in Figure 1.2, main Subsystems of proposed method are including the Vision Subsystem, the Path Planning (APF+Visual Servoing (VS)) Subsystem, the Kinematic Model Simplification Subsystem, and the Velocities Planning Subsystem

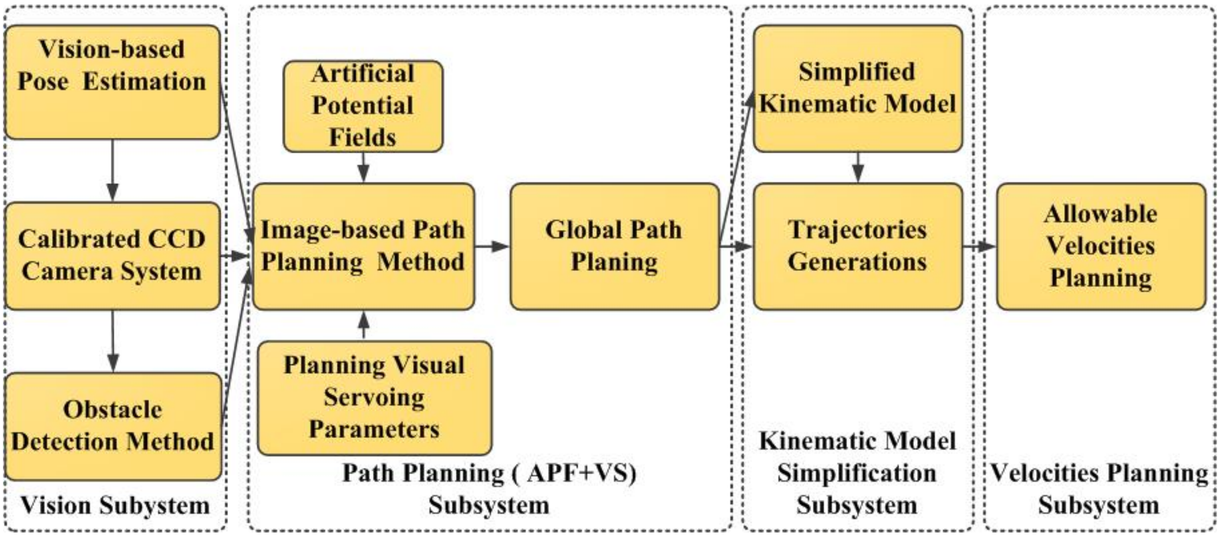

Figure 1.2: Scheme of the proposed vision-based trajectory generation for mobile robots with steerable wheels through only one camera.

As illustrated in Figure 1.2, the block diagram of the proposed vision-based method has four main following parts:

- The Vision Subsystem consists of the functions that process the grabbed images by calibrated Charge Coupled Device (CCD) camera, estimate the desired poses and detect the obstacles.

- The Path Planning (APF+VS) Subsystem is the main part of this method that defines the relationship between the motion of a robot in the world coordinates and the corresponding motion in the image space. Flowchart of this Subsystem and its related software/hardware are shown in Figure 1.3.

- The Kinematic Model Simplification Subsystem generates the trajectories for all the wheels which simplify the complexity of kinematic model of the robot.
- The Velocities Planning Subsystem is used for planning maximum allowable linear and angular velocities using the kinematic variables which come from the previous Subsystem.

In this study, Matlab is used for vision-based path planning and implementing the obstacles recognition tasks in the image space. Halcon (2007) software is employed to estimate the pose of the desired points using Computer-Aided-Design (CAD)-based recognition method which was proposed by Ulrich et al. (2009) in the initial and the desired robot configuration workspace. As illustrated in Figure 1.3, the robot motion in the world coordinates can be interpreted as the motion of the robot projected points in Two-dimensional (2D) image space that are under the influence of the defied APF. The APF has the positive charge in the initial pose and negative charge in the desired pose. Moreover, the recognized points of the obstacles in the image space are set with positive charges. The gradient field in this context can be interpreted as a force that attracts the positively charged mobile robot points to the negative points, which are acting as the goal.

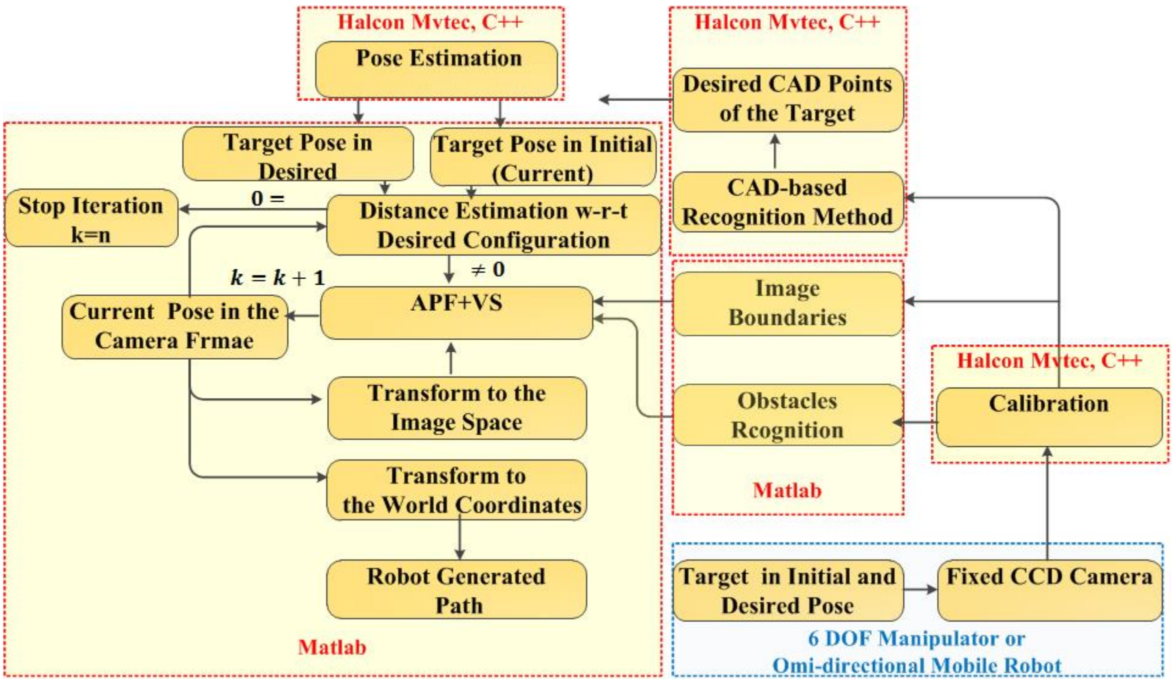

Figure 1.3: Flowchart of the Path Planning (APF+VS) Subsystem and its related software/hardware define the relationship between the motion of a robot desired points in the image space and corresponding motions in the world coordinates.

The obstacle points and the image borders act as a set of positive charges that generate repulsive forces in the image space to push the robot platform away from obstacles. Hence, the combination of attractive and repulsive forces drives the robot in a safe path to reach its desired pose. The VS functions define the relationship between the generated motion in the robot coordinates and corresponding motion in the image space with respect to the camera frame. The generated path can be transformed to the real world coordinates. The vision-based trajectory planning method generates synchronized trajectories for all of the wheels on 4WS mobile robots. Omni-directional mobile robots have the ability to move concurrently and independently in rotation and translation in the plane. For other types of robots, more mechanical constraints have to be employed to generate a suitable obstacle-free path.

This kind of vision-based path planning method deals with some main restrictions. Pose estimation accuracy, obstacles recognition problems, and the error in camera calibration can effect the subsequent processing which compromises highly on the overall accuracy of the system. As explained by Thomas (2008), accuracy of the pose estimation results cannot be defined in absolute sense because the CAD-based recognition problem is too loosely defined. The pose estimation approach has two major parts including object modeling and object matching. Most existing Three-dimensional (3D) object modeling approaches construct the object model using object geometric models that can be obtained either manually or by learning from multiple images of an object.

Obstacle detection has a large variety of approaches due to the different shapes, sizes, and orientations of obstacles with respect to the camera's position. In vision-based methods of detecting obstacles, a single camera or a stereo camera is usually used. Methods based on stereo vision are fundamentally limited by the finite baseline between the stereo pairs, and fail in presence of specular reflections and textureless regions. In the case of using a single camera, it is necessary to keep the camera at a higher position in order to acquire higher accuracy of measuring the distance from obstacles Iwata et al. (2002).

Another restriction on direct usability of the proposed method is the limitation of experimental testing time in such hazardous environments. In Divertor Cassette Preloading Tool task as a case study, the high degree of freedom water hydraulic manipulator called WHMAN is installed on top of a mobile platform in order to reach the required robot workspace. Therefore, the desired pose to be reached by the end-effector is partially unknown with respect to the robot-base. However, in experimental tests, we assume that 6 DOF robot manipulator called Comau Smart NM $45-20$ is mounted on top of the platform. Therefore, the relative desired pose of the end-effector with respect to the robot-base can change in each round of the RH task. The major problem in the path planning method using the APF is the local minimum issue that can create a trap for the robot before it reaches its destination. However, as proposed by Warren (1989), by considering the entire off-line path, the local minimum problem is greatly reduced to allow the method to be used for global path planning.

1.3 Contribution of the Present Research

The thesis contributions are centered on the following lines of research:

- Most RH systems in hazardous and inaccessible to human environments such as ITER, have to tackle the lack of visual feedback for human operators due to limited on-site cameras, occlusion, poor viewing angles, and etc. To solve this problem, in [**P1**], vision-based markerless AR method is presented. As a case study, this method enables the user for recognizing and positioning the markerless manipulator tool in near real-time for the Water Hydraulic Manipulator (WHMAN) Divertor Cassette Preloading Tool task in the ITER reactor. This method can also be used to enhance user's understanding of the situation of moving objects in 3D space to detect the presence or absence of the moving object.

- In [**P2**], path planning method is presented for manipulation task by integrating the defined APF, VS concepts, and CAD-based recognition method while the camera is mounted on the robot's end-effector. The generated path must stay in the camera's field of view during the operation while not losing its robustness.
- The expected level of radiation in a nuclear environment such as ITER reactor, induces the incorporation of RH techniques for inspection, and maintenance tasks. To increase the performance of such highly intricate systems, an assistive new vision-based method is presented in [**P3**] for controlling the manipulation tasks remotely. The generated 6D paths have the potential to reduce operator stress and increase system performance by visualization the 3D position and 3D orientation of the target using a color cue (red, blue, green), and displaying the generated path with respect to the camera frame.
- In [**P4**], we extend our previous work in [**P3**] to present a new global and obstacle-free path planning method for omni-directional mobile robots with steerable wheels relying only on one overhead camera. The proposed algorithm is able to find the safe path through hazardous and confined workspaces while the generated path is entirely within the image boundaries.
- In [**P5**], the new relation between the generated path for the 4WS mobile robot in the image space and the corresponding generated trajectories in the world coordinate is defined. We extend our previous work in [**P4**] to present a novel method for generating synchronized trajectories for all the steerable wheels on mobile robot. These generated synchronized trajectories are used to reduce the complexity of the mobile robot kinematic model to plan the maximum bounded velocities for mobile robots.
- In [**P6**], we extend our previous work in [**P5**] to present a new vision-based method for coordinating multiple mobile robots with 4WS in a confined shared workspace to avoid mutual collisions. The major problem with this type of mobile robots is their relative complexity in the kinematic and dynamic models and the need to design separate controllers for each robot's position and orientation.

This thesis comprises two parts. The first one is an introductory part, while the second one consists of six publications. The structure of the first part is as follows: Chapter 2 reviews the state-of-the-art in topics that are relevant to meeting the objectives of this thesis. Chapter 3 presents a summary of the publications, and Chapter 4 presents the conclusions of the thesis.

1.4 Author's Contribution to the Publications

This section clarifies the author's contribution to the published work.

P1 The author wrote the paper and developed the methods presented in the paper. Antti Hahto helped with the experimental implementation and reviewed the paper. Luigi Semeraro, Mikko Siuko and Professor Jouni Mattila helped with use case definition, reviewed the paper and made corrections and suggestions.

P2 The author wrote the paper and developed the new scheme for image space path planning presented in the paper. Reza Oftadeh helped with the experimental implementation and reviewed the paper. Professor Jouni Mattila reviewed the paper and made corrections and suggestions.

P3 The author wrote the paper and developed the obstacle-free path planning method. Reza Oftadeh helped with the experimental implementation and reviewed the paper. Professor Jouni Mattila reviewed the paper and made corrections and suggestions.

P4 The author wrote the paper and developed the global path planning with obstacle avoidance method presented. Reza Oftadeh helped with the experimental implementation of the method with omni-directional mobile robot and reviewed the paper. Professor Jouni Mattila reviewed the paper and made corrections and suggestions.

P5 The author wrote the paper and developed the vision-based trajectories planning method presented. Reza Oftadeh provided the kinematic model and helped with the experimental implementation of the method with omni-directional mobile robot and reviewed the paper. Professor Jouni Mattila reviewed the paper and made corrections and suggestions.

P6 The author wrote the paper and developed the vision-based path coordination for multiple mobile robots presented. Reza Oftadeh helped with the experimental implementation of the method with omni-directional mobile robot and reviewed the paper. Professor Jouni Mattila reviewed the paper and made corrections and suggestions.

2 Review of the State-of-the-Art

The main objective of this chapter is to review the state-of-the-art that has been identified as relevant to meeting the objectives of this thesis.

The computer vision applications in robotics that focus in pose estimation and obstacle avoidance methods using CCD camera are presented in Section 2.1. A short overview on VS concepts that are required in this thesis is addressed in Section 2.2. Then, the state-of-the-art knowledge in conventional path planning and trajectory generation methods introduced in Section 2.3. Finally a summary of the presented state-of-the-art is explained in Section 2.4.

2.1 Computer Vision Applications in Robotics

Computer vision studies examine how to understand, reconstruct, and interpret a 3D scene from a 2D image using the properties of the structures present in the scene. Human vision is limited mainly by memory, the visible spectrum, and illusion. The main goal of computer vision systems is to exceed human vision using computer hardware and software utilizing different types of knowledge in computer science, mathematics, electrical engineering, and so forth. Computer vision has a wide range of applications in the field of robotics, such as mobile robots positioning and navigation, see Figure 2.1. This section focuses on the computer vision applications in pose estimation and obstacle avoidance using CCD camera.

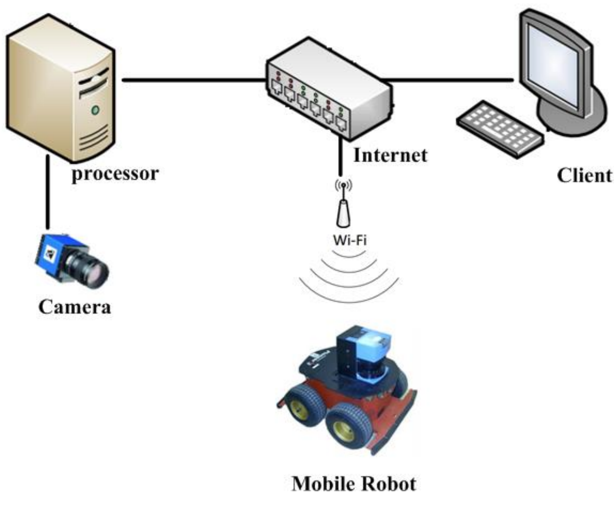

Figure 2.1: Mobile robot navigation is a critical component in creating truly autonomous systems. Computer vision applications plays a major role in developing improved and robust navigation algorithms.

2.1.1 CCD Camera System

A “pinhole” CCD camera provides a perspective projection of a 3D point on the image plane. The image plane is a matrix of light sensitive cells. The resolution of the image is the size of the matrix. A single cell is called a “pixel”. For each pixel of coordinates $(u, v)^T$, the camera measures the intensity of the light. The perspective projection of a world point into pixel row and column coordinate $(r, c)^T$ is explained as follows. We consider a CCD camera with a field of view that covers the desired workspace W. Let the known point $P^W = (x_w, y_w, z_w)^T$ in the world coordinates is transformed into point $P^C = (x_c, y_c, z_c)^T$ of the camera coordinates using the transformation comprising of rotation R and translation t.

$$\begin{pmatrix} P^C \\ 1 \end{pmatrix} = \begin{bmatrix} R & t \\ 0 & 1 \end{bmatrix} \begin{pmatrix} P^W \\ 1 \end{pmatrix}. \tag{2.1}$$

For pinhole camera model, this point $P^C = (x_c, y_c, z_c)^T$ in the camera coordinates projected to the image plane coordinates $(u, v)^T$ via perspective transformation by following equations:

$$u = \frac{f}{z_c} x_c,$$
$$v = \frac{f}{z_c} y_c, \tag{2.2}$$

where (u, v) are image plane coordinates and (x_c, y_c, z_c) are orthogonal camera center coordinates, and f is the focal length. In presence of radial distortion, the lens distortion converts the image projection point (u, v) into the camera image plane $(\widetilde{u}, \widetilde{v})$. In CCD calibration process, division model uses parameter k to model the radial distortion. Using the following equations, the distorted image plane coordinates can transform into undistorted image plane coordinates:

$$u = \frac{\widetilde{u}}{1 + k(\widetilde{u}^2 + \widetilde{v}^2)}$$

$$v = \frac{\widetilde{v}}{1 + k(\widetilde{u}^2 + \widetilde{v}^2)}. \tag{2.3}$$

The lens distortion can convert the image projection point (u, v) into the camera image plane $(\widetilde{u}, \widetilde{v})$ using the following equations Steger et al. (2008):

$$\widetilde{u} = \frac{2u}{1 + \sqrt{(1 - 4K_1(u^2 + v^2))}},$$
$$\widetilde{v} = \frac{2v}{1 + \sqrt{(1 - 4K_1(u^2 + v^2))}}, \tag{2.4}$$

where, K_1 is the distortion coefficient. The transformation point from the image plane coordinates into the image center coordinates system with column c and row r in the image space are:

$$c = \frac{\widetilde{u}}{S_x} + C_x,$$

$$r = \frac{\widetilde{v}}{S_y} + C_y, \tag{2.5}$$

where C_x and C_y denote the column and the row coordinates of the image center of the radial distortion and S_x and S_y are the camera scale factors.

As explained above, we obtain the required camera calibration parameters in presence of radial lens distortion. These parameters are required for pose estimation in [**P1**]-[**P6**]. Furthermore, by utilizing these parameters, the visual servoing variables such as end-effector velocity screw and Jacobian matrix are calculated. These concepts will be explained in Section 2.2.2. In [**P2**], the Jacobian matrix is required to calculate repulsive potential forces whit respect to the camera frame while the camera is mounted on robot's end-effector. In [**P4**]-[**P5**], we calculate the image Jacobian matrix to obtain desired repulsive forces while the mobile robot is moving under the fixed overhead camera.

2.1.2 Vision-based Pose Estimation Methods

This section provides an overview of methods in vision-based pose estimation techniques. It is straightforward to mathematically describe the process of projection from a 3D scene model to a 2D image, but the inverse problem is considerably more difficult. The physical world is three-dimensional, but a camera's image contains only a two dimensional projection of this reality. In the physical world, a pose is defined as position and orientation of the camera in relation to 3D structure. The most straightforward method for pose estimation is to derive the analytical transformation between the projected object's points on the 2D image plane and their 3D pose by employing the known relationship between the object points themselves and the projection model of the camera.

Pose estimation methods can be classified roughly by the following estimation approaches: dimension of the model used (2D-2D, 3D-3D, 2D-3D), image feature types (edge, plane, etc.), and the recognition process (aspect graph, etc.). Closed form least-squares solutions, a globally convergent iterative technique and a simplified linear solution are presented by Haralick et al. (1989) for 2D-2D pose estimation problem. In some presented methods such as ARToolkit Kato and Billinghurst (1999), the object's rotation and translation can be estimated by calculating the inter-frame displacement of the current image with respect to the reference template. Lucas et al. (1981) used optical flow approach to estimate the pose in consecutive 2D images that is suitable for the planar objects with textures.

In vision-based 3D-3D pose estimation method, the data sets consist of three-dimensional data points in a three-dimensional space. For example, when a 3D object is viewed with a stereo camera system, one set data is the metric CAD model, and the other is a 3D point cloud that is retrieved via the stereo camera system. The corresponding pairs of points can be obtained by matching process. Then the desire pose can be estimated with different proposed method, for example Iterative Least Squares Solution proposed by Haralick et al. (1989) or a registration method called RANdom SAmple Consensus (RANSAC) algorithm developed by Fischler and Bolles (1981).

The 2D image should show the points of the 3D object, which is called 2D-3D correspondences. The problem of object pose from 2D to 3D correspondence has received a lot of attention in the computer vision literature, for instance Simo-Serra et al. (2013), Gold et al. (1998), and Horaud et al. (1997). Most of the algorithms are based on linear or nonlinear equations to be solved with different methods. For example Perspective n-Point method for 2D-3D with n feature points presented by Fischler and Bolles (1981). Figure 2.2 shows the flowchart of 3D model-based pose estimation methods. The goal is to find the correct pose of the 3D model which rendered will match as best as possible with the input image. Methods based on stereo camera set-up are fundamentally limited by the finite baseline between the stereo pairs and fail in textureless regions and in presence of specular reflections. The 2D-3D pose estimation by initial iterative solution was proposed by Haralick et al. (1989). Vision-based 2D-3D pose estimation method, calculate the desired pose mainly by matching the re-projection 3D model of the object and its corresponding features in the image. The CAD-model or geometric information is necessary to compute the required pose.

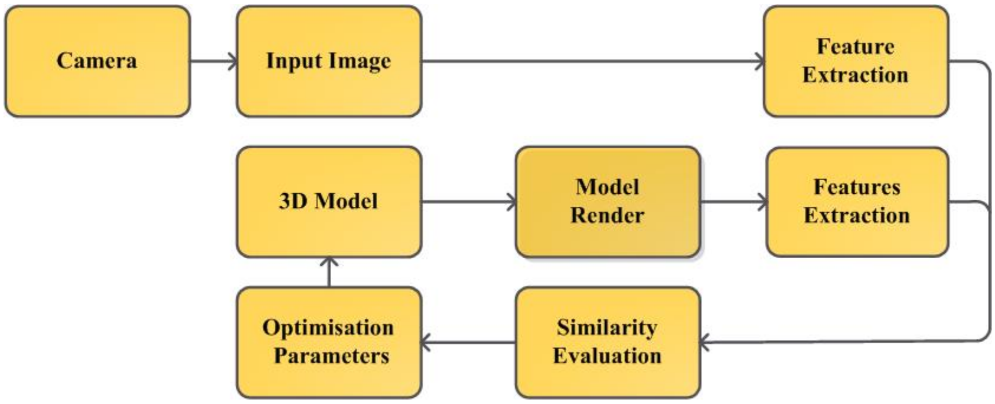

Figure 2.2: This flowchart shows the main levels of 3D model-based pose estimation approaches. 3D model-based pose estimation can be divided into two different types of methods depending on the image features used to evaluate similarity between the rendered model and the input image.

To estimate the position and orientation of the 3D object using only one camera, the following methods are proposed:

- **Virtual Visual Servoing Pose Estimation**: Comport et al. (2006) proposed a method for pose computation and camera displacement estimation and its formulation in terms of full scale nonlinear optimization that is called Virtual Visual Servoing (VVS). The pose-estimation problem is considered as similar to the 2D VS problem. Essentially, 2D VS consists of specifying a task, such as position tracking as the regulation in the image of a set of visual features. Then, a closed-loop control law minimizes the error between the current and desired position of these visual features which can be implemented to determine the motion of the camera has to realize. The proposed approach is stable for lighting changes. However in highly textured objects with a cluttered background, the desired edges cannot be detected correctly, which is the main limitation of the proposed method. Furthermore, if the initial pose error is large, i.e. when the object is far from the initial pose, then this approach can have difficulties in finding the right pose.
- **POSIT Algorithm**: Dementhon and Davis (1995) proposed an algorithm called Pose from Orthography and Scaling with ITeration (POSIT) for computing the object's pose (translation and rotation) described by six parameters $(x, y, z, \alpha, \beta, \gamma)$. This pose estimation algorithm can estimate the position and orientation of known objects in three dimensions with respect to a camera frame from 3D to 2D point correspondences. Indeed, in this proposed method, linear resolution methods can be used to obtain only a pose approximation. Non-linear resolution methods lead to a very accurate solution, but proper initialization is required. Based on the POSIT algorithm, we must find the corresponding location of at least four non-coplanar

feature points on the surface of the object in the image. The POSIT algorithm can be written mathematically in 25 lines or less. Therefore, it can be a very useful method for near real-time operation. Open CV functions for the POSIT algorithm are presented by Bradski and Kaehler (2008) to simplify the pose estimation of 3D objects in a single image.

- **CAD-based Pose Estimation Method**: Recently, there has been an increasing interest in utilizing 3D models for object recognition and pose estimation. 3D object recognition and pose estimation in images are difficult and important problems in computer vision. A 3D object recognition method has two major parts including object modeling and object matching. Most 3D object modeling approaches construct the object model using object geometric models that can be obtained either manually or by learning from multiple images of an objects. CAD-based techniques address these issues by taking the advantage of a prior knowledge of the object whose pose and motion are to be estimated Ulrich et al. (2009). Pose estimation approaches with the CAD model try to search within the entire possible 6 DOF pose space to find the best match between rendered computer graphic images and an image of the real scene. As illustrated in Figure 2.3 the geometric 3D CAD model of the 3D target are necessary to extract 3D pose information from a single image. If the intrinsic parameters of the camera are known, we still have to estimate at least 6 parameters for translation and rotation to determine the exact pose of the model. This 3D knowledge typically consists of a CAD description of the object in the form of a CAD model of the object incorporating known structures, shapes, textures, transmittance, or other visual attributes.

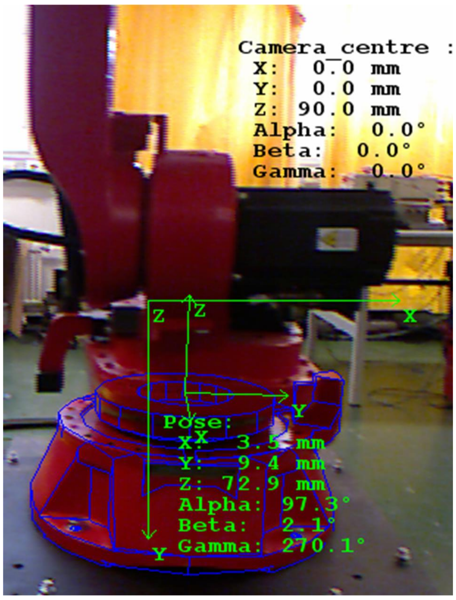

Figure 2.3: To estimate the pose of the robot-center coordinates with respect to the fixed camera frame, we employ the created CAD model of the robot's base (Comau Smart) while CAD's center frame coincides with the robot-center coordinates.

In this thesis, to estimate the position (x, y, z) and orientation (α, β, γ) of a mobile robots or a manipulator's end-effector in initial and desired pose, we employ the CAD-based recognition method proposed by Ulrich et al. (2009). This method is robust to occlusion, clutter, and lighting that make it desirable especially for vision guided robotics.

2.1.3 Vision-based Obstacle Avoidance

One of the key research problems in robotics is the developments of obstacle avoidance methods. To cope with this problem, most autonomous navigation solutions rely on range data by utilizing laser rangefinders and stereo vision techniques to estimate the range or distance from the image to the robot. However, these methods have some drawbacks. For instance, laser range finders are expensive and stereo vision systems have vast amount of computational complexity that consumes computation time.

Vision-based obstacle avoidance methods are classified into two main groups: methods that rely on the apparent motion which is called optical flow based technique Guzel and Bicker (2010), and methods that rely on the appearance of individual pixels for vision-based methods using only one camera Ulrich and Nourbakhsh (2000). In this method, the classification of the obstacles was carried out using the pixel difference between the template and the active image patterns. This method assumes that the color of obstacle differs from the reference region, and the pixel whose color is not included in the reference region is detected as an obstacle. However, most of these methods are very time consuming to execute. However, for appearance-based obstacle detection, the following assumptions are required for a variety of indoor and outdoor environments:

- Obstacles must differ in appearance to enable the robot to distinguish the obstacle from the ground.
- The ground should be relatively flat.
- No overhanging obstacles should be present.

The last two assumptions allow us to estimate the distance between a detected obstacle and the camera. This pixel classification represents an obstacle or the ground based on a number of local visual attributes, such as intensity, color, edges, and texture. Objects to be detected in a scene can have a large variety of appearances due to different shapes, sizes, and orientation with respect to the camera's position. Combined with a cluttered background and a range of visibilities under various lighting conditions, the solution for a reliable and accurate algorithm requires complicated system configurations and extensive evaluation.

In this thesis, we use color information as our primary cues to detect the obstacles. Color has many appealing attributes for mobile robots navigation. For instance, Turk and Marra (1987) proposed an obstacle-avoidance algorithm that uses color cues instead of edges to detect obstacles on roads with minimal texture. This method detects obstacles by subtracting two consecutive color images from each other. Knowing of the robot's or the obstacle's motion is necessary requirement in this method. Compared to texture, color is more local attribute can be calculated much faster. In addition, color provides more information than intensity alone. In order to segment out obstacles or any marker belonging to them, color thresholds are first defined by sampling pixel values offline for each marker in a robot's workspace. Simple color thresholding produces a series of binary masks indicating presence or absence of each marker's color at every pixel. To eliminate noise, one pass of erosion or dilation using a rectangular structuring element is performed. Finally, a step of connected components labeling is applied to group pixels corresponding to the same marker.

Several models are available for representing color, such as the Red, Green, Blue (RGB) model. However, color information for the RGB model is very noisy at low intensity. The

RGB format is mostly converted to Hue, Saturation, Value (HSV) and Hue, Saturation, Intensity (HSI). In the HSV method, Hue is what humans perceive as color, S is Saturation and Value is related to brightness. In the HSI model H and S represents the same as the parameters in the HSV color model, but I is an intensity value with a range between [0,1], where 0 is black and white is 1. These color spaces are assumed to be less sensitive to noise and lighting conditions. The flowchart of the appearance based obstacle detection system is illustrated in Figure 2.4. In this approach, the input image is convolved with a smoothing filter to reduce the noise effects, and then the smoothed image is converted to HSI or HSV or any related color space. Most vision-based methods detect specific obstacles according to the characters of the obstacles, such as shape, color, intensity, and so on. Static unknown obstacle segmentation in realistic cluttered manipulation scene using only one CCD camera still is not feasible.

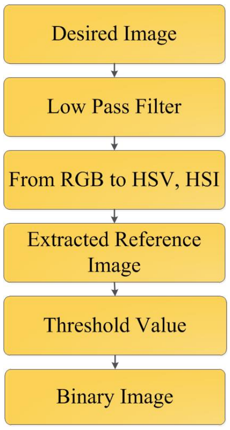

Figure 2.4: Appearance-based object (obstacle) detection using the color cues algorithm.

In publications [**P3**] − [**P6**], we use color information as our primary cue to detect obstacles. Autonomous robot collision avoidance requires an accurate separation of obstacles from the background. Numerous vision-based detection and segmentation approaches have been proposed. Image segmentation refers to the process of segmenting the pixels from an image into a region. An image can be segmented into regions in order to find objects or boundaries of the object. To this end, the obstacles are segmented using the HSV color filter method, proposed by Sural et al. (2002). These types of methods basically consist of detecting pixels that are different in appearance on the ground and then classifying them as obstacles.

2.2 Vision-based Robot Control

This section provides a brief overview of Visual Servoing concepts that concerns several fields of research including image processing, computer vision, robotics, and control theory. VS schemes can be classified based on the knowledge we have about the target and the camera parameters. If a camera is mounted on robot's end-effector, it is called "camera-in-hand." If the camera observes the robot from a fixed position, the system is called "camera-to-hand" or "camera-out-hand." In a hybrid system, both cameras systems are employed. The use of VS system allows the operator to carry out point-to-point motion of a robot using visual information. VS systems can be divided into PBVS and Image-based Visual Servoing (IBVS). In PBVS, features are extracted from the image to determine the pose of the target with respect to the camera frame by utilizing a model of the target. The calibrated vision system is used to estimate the relative pose of the target with respect to the end-effector. In the IBVS method, pose estimation is omitted and the robot control law is expressed directly in the image space. Both methods have advantages and disadvantages. For example, the position-based methods are better for large range measurements, and image-based techniques are more suitable for small range measurements.

This thesis focuses on issues related to those specific geometric aspects of computer vision that are relevant to the study of robot control and issues related to 3D pose estimation. To define the VS concepts in 3D Cartesian space, we consider the task space of the robot, represented by τ which is the set of positions and orientations that the robot tool can attain. If the tool is a single rigid body moving arbitrarily in a 3D workspace, then: $\tau = SE^3 = \Re^3 \times SO^3$, where three-dimensional Euclidean space is denoted by $\Re^3$ and the possible rotational symmetries of an object is denoted by SO^3. The goal of the VS system is to minimize an error $\mathbf{e}$ between the current value of the visual feature $\mathbf{s}$ and its desired value $\mathbf{s}^*$ as follows:

$$\mathbf{e} = \mathbf{s} - \mathbf{s}^* \tag{2.6}$$

In VS applications, we are interested in the relationship between the velocity of desired object and the corresponding changes that occur in the observed image. If the end-effector is moving in a workspace with $\tau \subseteq SE^3 = \Re^3$, this motion is described in an angular velocity $\mathbf{\Omega}(t) = [\omega_x(t), \omega_y(t), \omega_z(t)]^T$ and a translational velocity $\mathbf{T}(t) = [T_x(t), T_y(t), T_z(t)]^T$ with respect to the robot base coordinates. Let $\mathbf{P}$ be a point that is rigidly attached to the robot end-effector, with base frame coordinates denoted by $[x, y, z]^T$. Then, the time derivatives of the coordinates of $\mathbf{P}$ defined in the robot base frame coordinates are given via following equations:

$$\begin{aligned} \dot{x} &= zw_y - yw_z + T_x, \\ \dot{y} &= xw_z - zw_x + T_y, \\ \dot{z} &= yw_x - xw_y + T_z. \end{aligned} \tag{2.7}$$

Then we can write these three equations as the following relation:

$$\dot{\mathbf{P}} = \mathbf{\Omega} \times \mathbf{P} + \mathbf{T}. \tag{2.8}$$

We assume parametrization task space $\mathbf{r} = [x, y, z]^T$ refers to the position of the end-effector. Together, $\mathbf{T}$ and $\mathbf{\Omega}$ define velocity screw $\dot{\mathbf{r}}$:

$$\dot{\mathbf{r}} = \begin{bmatrix} T_x \\ T_y \\ T_z \\ \omega_x \\ \omega_y \\ \omega_z \end{bmatrix}, \tag{2.9}$$

where $\dot{\mathbf{r}}$, represents the derivative of vector $\mathbf{r}$. The most commonly used VS controller is the velocity controller. To design this controller, we need the relationship between the time variation of $\mathbf{s}$ and the camera velocity denoted by $\mathbf{V_c} = (\upsilon_\mathbf{c}, \omega_\mathbf{c})$, where, $\upsilon_\mathbf{c}$ is the instantaneous linear velocity of the origin of the camera frame and $\omega_\mathbf{c}$ is the instantaneous angular velocity of the camera frame mounted over the end-effector. Image Jacobian

$\mathbf{L_s} \in \mathbf{R}^{k\times 6}$ is called the interaction matrix which is related to $\mathbf{s}$ and plays a crucial role in the controller design with the following form:

$$\dot{\mathbf{s}} = (\frac{\partial \mathbf{s}}{\partial \mathbf{r}})(\frac{\partial \mathbf{r}}{\partial t}) = \mathbf{L_s V_c}, \tag{2.10}$$

where $\frac{\partial \mathbf{r}}{\partial \mathbf{t}} = \mathbf{V_c}$ is the camera velocity screw that represents the translational and rotational components of the camera. Therefore, we can obtain the relationship between camera velocity and time variation of the error using equations (2.6) and (2.10):

$$\dot{e} = \mathbf{L_e V_c}, \tag{2.11}$$

where $\mathbf{L_e} = \mathbf{L_s}$ and $\mathbf{V_c}$ is the input to the robot controller and $\dot{\mathbf{e}} = -\lambda \mathbf{e}$ we have:

$$\mathbf{V_c} = -\lambda \mathbf{L_e^+} e, \quad \mathbf{L_e^+} \in \mathbf{R}^{k\times 6} \tag{2.12}$$

As described by Malis et al. (1999), using equation (2.11), we can obtain the following equation:

$$\dot{\mathbf{e}} = -\lambda \mathbf{L_e} \widehat{\mathbf{L_e^+}} e \tag{2.13}$$

where $\mathbf{L_e^+}$ is chosen as pseudo inverse of $\mathbf{L_e}$. This is the basic design implementation for PBVS and IBVS controllers.

2.2.1 Position-based Visual Servoing

In PBVS, feature vector $\mathbf{s}$ is extracted from the image and used to estimate the pose of the target with respect to the calibrated camera frame. Computing this pose from a set of measurements in the image necessitates that the camera intrinsic parameters and the geometric 3D model of the object observed are known. PBVS system allows the direct and natural specification of the desired relative trajectories in the end-effector Cartesian coordinate frames. Therefore, the main advantage of PBVS is that the desired tasks can be described in Cartesian space, which is commonly used in robotics. While the estimation of the quantity of positions is a function of the system calibration parameters, the PBVS task can become extremely sensitive to calibration error. Figure 2.5 shows a basic model of the PBVS system.

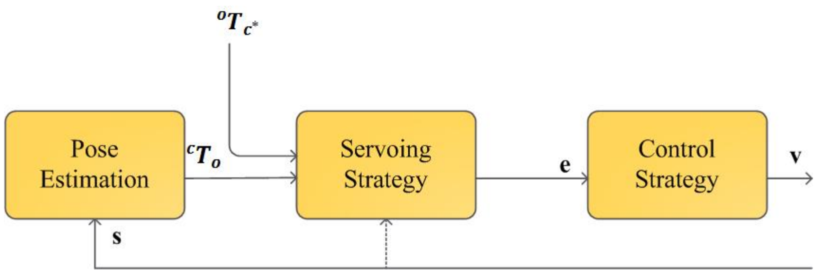

Figure 2.5: A general model of visual servoing system which can be used with most PBVS approaches. This model refers a servoing control since image measurements are used to determine the pose of the target with respect to the camera frame. It is based on camera-in-hand configuration, and the objective of servoing is defined as bringing the camera to a desired position with respect to the target.

This system has three parts: Pose Estimation, Servoing Strategy, and Control Strategy which are based on camera-in-hand configuration. The goal is to bring the camera that is mounted on robot's end-effector to the desired pose with respect to the target Kyrki et al. (2006). **s** denotes image measurement and ${}^{O}T_{C^*}$ denotes the rigid body transformation (position and orientation) to a measured desired object. ${}^{C}T_O$ shows the current measured pose of the object with respect to the camera. The pose estimation system can compute the position and orientation of the 3D target using the methods explained in the Section 2.1.2. The Servoing Strategy is based on the modeling of an error function. The Control Strategy such as a proportional control law affects the error convergence properties, especially when the target is moving.

As illustrated in Figure 2.6, three coordinate frames including the current camera frame $\mathcal{F}_C$, the desired camera frame $\mathcal{F}_C^*$, and a reference frame $\mathcal{F}_O$ are attached to the object. In PBVS, the task function is defined in terms of the pose transformation between the current and desired pose, which can be expressed as the transformation ${}^{C^*}T_C$. The input image is usually used to estimate the transformation ${}^{C}T_O$. Thus, the coordinate vectors ${}^{C}t_O$ and ${}^{C^*}t_O$ give the coordinates of the origin of the object frame expressed with respect to the current camera frame C and relative to the desired camera frame C^*, respectively.

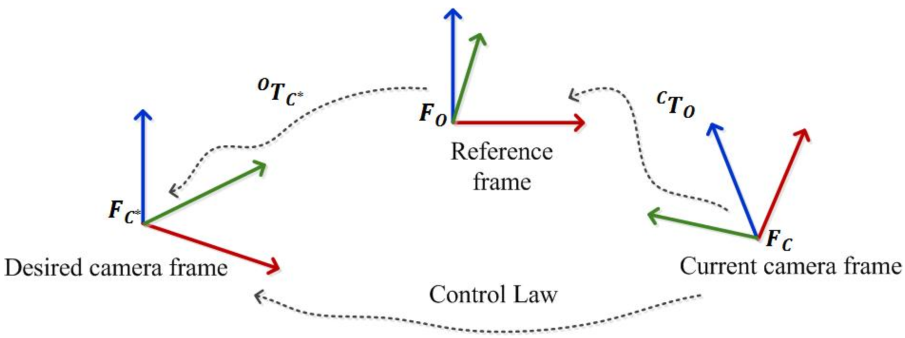

Figure 2.6: Coordinates of the PBVS system including the current camera frame, the desired camera frame, and the reference frame

Let **s** is $(t, \theta\mathbf{u})$, where t is a translation vector, and $\theta\mathbf{u}$ is the angle/axis parameterization for the rotation. Therefore, if t is defined with respect to the frame $\mathcal{F}_O$, then $\mathbf{s} = ({}^{C}t_O, \theta\mathbf{u})$, $\mathbf{s}^* = ({}^{C^*}t_O, 0)$, and $\mathbf{e} = ({}^{C}t_O - {}^{C^*}t_O, \theta\mathbf{u})$. In this case, the interaction matrix related to **e** is given by

$$\mathbf{L_e} = \begin{bmatrix} -\mathbf{I}_3 & [{}^{C}t_O]_\times \\ 0 & \mathbf{L}_\theta\mathbf{u} \end{bmatrix}. \tag{2.14}$$

If **I** is the 3×3 identity matrix and $\mathbf{L}_\theta\mathbf{u}$ is given by Cervera et al. (2003) as follows:

$$\mathbf{L}_\theta\mathbf{u} = \mathbf{I}_3 - \frac{\theta}{2}[\mathbf{u}]_\times + (1 - \frac{sinc(\theta)}{sinc^2(\frac{\theta}{2})})[\mathbf{u}]_\times^2, \tag{2.15}$$

where $sinc(\alpha)$ is the sinus cardinal defined such that $\alpha sinc(alpha) = sin\alpha$ and $sinc(0) = 1$. Therefore we can obtain the control scheme:

$$\mathbf{V_c} = -\lambda\widehat{\mathbf{L_e}^{-1}}\mathbf{e}. \tag{2.16}$$

PBVS is based on the selection of a set of visual features **s** that has to reach a desired value $\mathbf{s}^*$. As explained above, **s** consists of a set of features that are available in the image data. $\mathbf{s}^*$ can be obtained either during an off-line learning step or by computing the projection in the image of a 3D model of the target for the desired camera pose.

2.2.2 Image-based Visual Servoing

The IBVS approach entails extracting vision data from an image acquired from a camera and computing the visual data obtained at the desired position of the robot. In both cases, IBVS and PBVS may use either a fixed camera or camera-in-hand configuration. The motion of the robot causes changes to the image observed by the vision system. In IBVS control, an error signal is measured in the image mapped directly to the actuator commands. IBVS approaches have become increasingly popular, largely due to the shortcomings of PBVS systems. The goal of IBVS systems is achieved when the error function **e** becomes zero.

For an IBVS system, the control law involves the mapping between image space velocities and velocities in the robot's workspace. To this end, it is necessary to define a relationship between changes in the image features of the moving object and changes in the position of the object. The image Jacobian is a linear transformation matrix that describes how image feature parameters change while the robot's pose changes.

In computer vision literature, an extracted image feature corresponds to the projection of a physical feature of the object with respect to the camera image plane. The set of n image feature parameters can be defined as a vector $\mathbf{s} = [s_1, s_2, ...s_k]^T \in \mathcal{F} \subseteq \Re^n$, where $\mathcal{F}$ represents the image feature parameter space and k is the number of extracted image features. Let $\mathbf{r}$ represents coordinates of the end-effector in desired parametrization of task space τ, and $\dot{\mathbf{r}}$ represents the corresponding velocity of the robot. We assume that $\mathbf{f}_e$ represents a vector of the image feature parameters and $\dot{\mathbf{f}}_e$ is the corresponding vector of image feature parameter rate of change. The image Jacobian $\mathbf{L}_f$ defines a linear transformation from the tangent space of τ at $\mathbf{r}$ to tangent space of $\mathcal{F}$ at $\mathbf{f}_e$ Castaño and Hutchinson (1994).

$$\dot{\mathbf{s}} = \mathbf{L}_f(\mathbf{s}, \mathbf{r})\dot{\mathbf{r}} \tag{2.17}$$

and

$$\mathbf{J}_v(\mathbf{s}, \mathbf{r}) = \left[\frac{\partial \mathbf{s}}{\partial \mathbf{r}}\right] = \begin{bmatrix} \frac{\partial s_1}{\partial \mathbf{r}_1} & ... & \frac{\partial s_1}{\partial \mathbf{r}_m} \\ . & ... & . \\ \frac{\partial s_n}{\partial \mathbf{r}_1} & .... & \frac{\partial s_n}{\partial \mathbf{r}_m} \end{bmatrix}, \tag{2.18}$$

where m is the dimension of the task space τ, and therefore, the number of Jacobian columns depends on the task. We assume $P = [x, y, z]^T$, then the derivative of the coordinates of P in terms of the image feature parameters u, v using equation (2.2) are:

$$\dot{x} = zw_y - \frac{v}{f}zw_z + T_x, \tag{2.19}$$

$$\dot{y} = \frac{v}{f}zw_z - zw_x + T_y, \tag{2.20}$$

$$\dot{z} = \frac{z}{f}(vw_x - uw_y) + T_z. \tag{2.21}$$

We have the following equation for $\dot{u}$:

$$\dot{u} = f\frac{z\dot{x} - x\dot{z}}{z^2} \tag{2.22}$$

$$\dot{u} = \frac{f}{z}T_x - \frac{u}{z}T_z + \frac{uv}{f}w_x + \frac{f^2 + u^2}{f}w_y - vw_z. \tag{2.23}$$

and similarly for $\dot{v}$.

$$\dot{v} = \frac{f}{z}T_y - \frac{v}{z}T_z + \frac{-f^2 - u^2}{f}w_x + \frac{uv}{f}w_y + uw_z. \quad (2.24)$$

Finally we have the following equations that relate the image-plane velocity of the object point to the relative velocity of the point with respect to the camera Malis et al. (1999).

$$\begin{bmatrix} \dot{u} \\ \dot{v} \end{bmatrix} = \begin{bmatrix} \frac{f}{z} & 0 & -\frac{u}{z} & -\frac{uv}{f} & \frac{f^2+u^2}{f} & -v \\ 0 & \frac{f}{z} & -\frac{v}{z} & \frac{-f^2-v^2}{f} & \frac{uv}{f} & u \end{bmatrix} \begin{bmatrix} T_x \\ T_y \\ T_z \\ \omega_x \\ \omega_y \\ \omega_z \end{bmatrix} \quad (2.25)$$

The Jacobian matrix is a function of z, therefore, estimation of z values for camera-in-hand can be more difficult than camera-to-hand. In a fixed camera system, when the target is a manipulator, the value of z, can be estimated using the forward kinematics. As explained in the Section 2.1.1, the lens distortion converts the image point projection (u, v) into the camera plane $(\widetilde{u}, \widetilde{v})$. Therefore, we can rewrite the linearized Jacobian matrices as:

$$\mathbf{L_s} = \begin{bmatrix} \frac{f}{z} & 0 & -\frac{\widetilde{u}}{z} & -\frac{\widetilde{uv}}{f} & \frac{f^2+\widetilde{u}^2}{f} & -\widetilde{v} \\ 0 & \frac{f}{z} & -\frac{\widetilde{v}}{z} & \frac{-f^2-\widetilde{v}^2}{f} & \frac{\widetilde{uv}}{f} & \widetilde{u} \end{bmatrix} \quad (2.26)$$

We can then write:

$$\dot{\mathbf{s}} = \mathbf{L_s V_c}. \quad (2.27)$$

To avoid a singularity, for 6 DOF robot end-effector, at least 3 feature points are required. The final interaction matrix is obtained by stacking the interaction matrices for all feature points.

$$\mathbf{L_s} = \begin{bmatrix} \mathbf{L_s}1 \\ \mathbf{L_s}2 \\ \mathbf{L_s}3 \end{bmatrix} \quad (2.28)$$

Singularities or poor conditioning in this Jacobian is a function of the relative position and motion of the camera and the object under observation that can lead to control problems. Since control is affected with respect to the image, there is no direct control over the Cartesian velocity of the robot end-effector.

In most of the VS schemes, the desired object may leave the camera's field of view during the servoing process, which leads to control failure. The failure may occur, because the feedback error cannot be computed anymore, the virtual link is broken, or the control loop cannot close. Different approaches have been developed to guarantee that the object remains in the camera's field of view during the robot or camera's motion. Morel et al. (2000) used a mixed 2D-3D approach and defined an ellipsis that includes all the features used in the reconstruction algorithm. They designed a control law to keep all the features in the image plane. Mezouar and Chaumette (2001) proposed an approach based on the use of potential fields in image space. Potential fields were employed by Corke and Hutchinson (2000) to retreat the camera's motion when the object features approach is in the boundaries of the image plane.

In [**P2**], VS concepts are used to define the relation between the motion of the 6 DOF end-effector and image extracted features of desired target while the camera is mounted on robot's end-effector. These concepts are used to define the proposed repulsive potential force that pushes the end-effector away from obstacles and visual constraints. The PBVS concepts are used in [**P3**] for vision-based path planning while the camera is mounted over the robot workspace. In [**P4**] – [**P6**], a combination of the PBVS and the IBVS concepts are used to define the image Jacobian matrix while the camera is fixed above the mobile robot's workspace. Furthermore, these concepts define the variation of robot coordinates to the variation of generated trajectory with respect to the fixed overhead camera to obtain the required repulsive potential fields and forces. A visibility constraint repulsive potential field implies a potential barrier function to push the mobile robot to reach the desired pose while remaining in the camera's field of view.

2.3 Conventional Path and Trajectory Planning Methods

Path planning is certainly one of the most interesting topics in advanced robotics and has been studied widely during the past few decades. It specifies the generation of a geometric path without a specified time law, while trajectory planning allocates a time law to the geometric path. As illustrated in Figure 2.7, path planning enables a high degree of robot autonomy for applications in hazardous environments, such as nuclear ITER reactor facilities, and CERN tunnels.

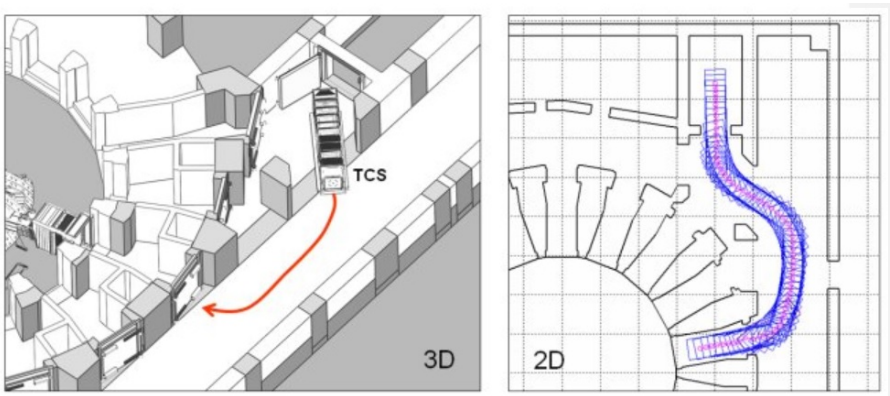

Figure 2.7: Path planning for mobile robots in cluttered environments with safety constrains in ITER reactor facilities. Approaches of path planning and trajectory optimization based on geometric constrains were studied and tested in the cluttered ITER scenarios by Vale and Ribeiro (2011)

Path planning is the problem of finding a geometric path from an initial configuration to a given terminating configuration such that each configuration is feasible. A geometric path consists of a set of configurations, where a configuration means a set of independent attributes which uniquely define the position and orientation of the mobile robot according to a fixed coordinates Eskandarian (2012). The general problem of path planning consists of searching for a collision-free motion between an initial and desired configuration. The path planning algorithm can sometimes be classified into two categories including planning in static environments and planning in dynamic environments. Planning in static environment assume that the position of the various obstacles do not change along with time.

The first step in the path planning process is to map the workspace into the robot configuration workspace C_{space}. The space of free configuration C_{free} determines the space that is obstacle-free for robot motion. In conventional path planning methods, configuration workspace is a multi-dimensional space limited by a set of generalized coordinates that describe the pose of a desired rigid body as a point. The planning problem is then reduced to moving the point representing the robot configuration from an initial to a desired configuration without entering any of the forbidden regions. The placement of a mobile robot is specified by a set of parameters that correspond to the number of degree of freedom a robot has. In 3D space, a robot with 3 DOF can only translate, but a robot with 6 DOF is free to translate and rotate. The four major approaches for mobile robot path planning include; road-map, cell-decomposition, graph-searching, and potential field. Each approach is briefly described as follows:

- Road-map approach is based on the capture of the free space connectivity on a system of one-dimensional curves in the C_{free} space, proposed by Bhattacharya and Gavrilova (2008). This built road-map is a set of standardized paths which can be reduced to linking an initial and a final configuration to a built road-map, see Figure 2.8.

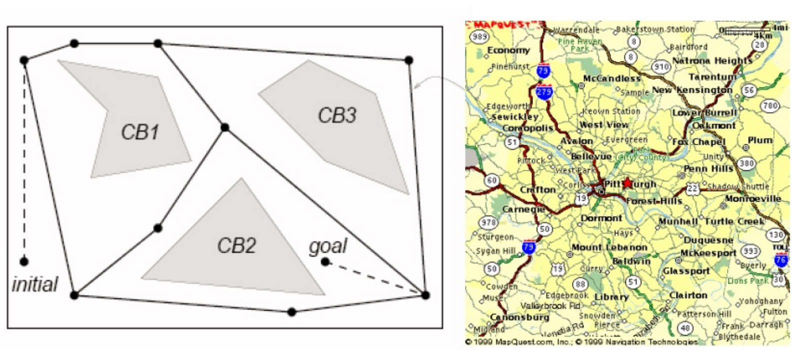

Figure 2.8: Basic path planning method by road-map methods.

- Cell-decomposition methods divide the free space of the robot in 2D Euclidean workspace in regions which called "cells." This makes it possible to easily create a connectivity graph between any two configurations of the same cell, which represent the adjacency relationships between the cells. Two types of cell decomposition methods are illustrated in Figure 2.9. The nodes of the graph represent the cells extracted from the C_{free}. Two nodes are connected by a link if and only if the corresponding cells are neighbors. From this connectivity graph, a continuous free path between initial and final configuration can be calculated, proposed method by Lingelbach (2004).

- The graph-searching method can be seen as applying a set of operators to the graph's nodes until the target nodes are found. It determines C_{free} spaces where no collision will occur and forbidden spaces where a collision will occur. Various implementations of graph search algorithms such as A* introduced by Goldberg and Harrelson (2005), D*, and focused D* proposed by Stentz et al. (1995) focus on strong points and drawbacks for each implementation and then a path is selected by merging the free spaces or by tracing around the obstacles.

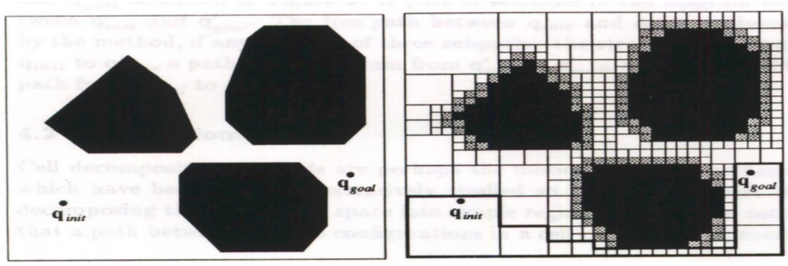

Figure 2.9: Exact cell decomposition (left) and approximate cell decomposition (right).

- A variety of potential field methods have been presented during the past decades that use the APF applied to the obstacles and desired pose. The most important advantages of this method are its easy extension to higher dimensions and the speed of the algorithm. The initial idea of using a potential field for robot path planning and obstacle avoidance was introduced by Khatib (1986). In past decades, potential field methods for manipulators and mobile robots have gained in popularity among robotics researchers. The idea represents the robot in the configuration space as a point moving under the influence of the potential that is produced by the objective configuration and the obstacles.

Path planning in image space using an artificial potential field was introduced by Mezouar and Chaumette (2000). In our configuration workspace in this thesis, each robot motion iteration is influenced by an artificial potential field. The influence of the artificial potential field V in the image space is the sum of the following two terms: 1) the attractive potential field V_{at}, whose role is to pull the robot toward the goal configuration $\boldsymbol{\Upsilon}$, and 2) the repulsive potential field V_{rp}, whose role is to push the robot away from constraints, such as obstacles. Typically, the target configuration generates a negative (attractive) potential field, while the obstacles are characterized by a positive (repulsive) potential field, see Figure 2.10.

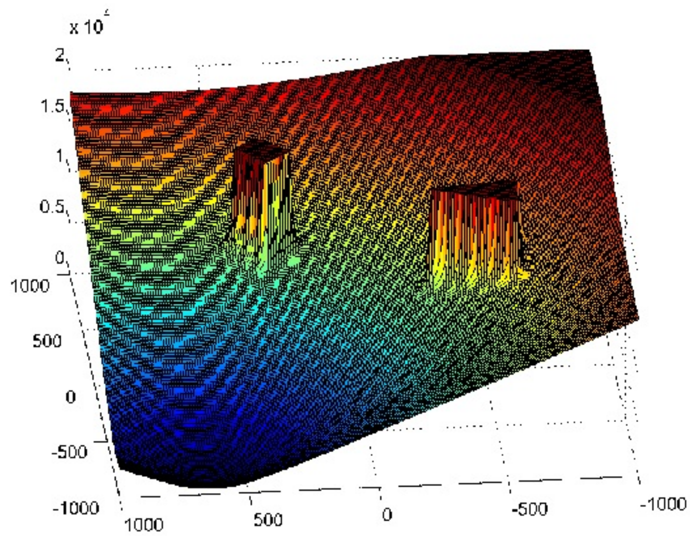

Figure 2.10: Total potential fields include negative (attractive) potential fields, while the obstacles are characterized by positive (repulsive) potential fields in desired scale.

Usually, the attractive and the repulsive potential fields are formulated separately, and the total potential fields of the workspace are obtained by linear superposition of both fields. The total potential field is obtained by adding the repulsive potential field resulting from obstacles in the workspace and the attractive potential field from the target. The artificial force $\mathbf{F}(\boldsymbol{\Upsilon})=-\vec{\nabla}V_{\boldsymbol{\Upsilon}}$ is the gradient vector of V at $\boldsymbol{\Upsilon}$. The initial configuration workspace is denoted by vector $\boldsymbol{\Upsilon}_j = [\mathbf{t}_j, (\mathbf{u}\theta)_j]$ and the desired configuration workspace is denoted by vector $\boldsymbol{\Upsilon}_d = 0_{6\times1}$. The vector $(\mathbf{u}\theta)$ is created using the axis and the angle obtained from the rotational matrix between the initial and desired poses.

$$\mathbf{F}(\boldsymbol{\Upsilon}) = \alpha\mathbf{F}_{at}(\boldsymbol{\Upsilon}) + \beta\mathbf{F}_{rp}(\boldsymbol{\Upsilon}), \tag{2.29}$$

where the attractive force is denoted by $\mathbf{F}_{at}(\Upsilon)$, the repulsive force is denoted by $\mathbf{F}_{rp}(\boldsymbol{\Upsilon})$, and $\boldsymbol{\Upsilon}$ is a 6×1 vector representing the parametrization of the robot workspace that is induced by potential fields. Scale factors α and β are used to adjust the influence of repulsive and attractive forces. The discrete time trajectory along the direction of $(\boldsymbol{\Upsilon})$ is obtained as follows Mezouar and Chaumette (2000):

$$\boldsymbol{\Upsilon}_{k+1} = \boldsymbol{\Upsilon}_k + \epsilon_k \frac{\mathbf{F}(\boldsymbol{\Upsilon}_k)}{\parallel \mathbf{F}(\boldsymbol{\Upsilon}_k) \parallel}, \tag{2.30}$$

where ϵ_k is a positive scaling factor and k is an index that increases during the generation of a path. The attractive potential field V_{at} is a parabolic function pulling the robot goal configuration to minimize the distance between the current and desired pose in 3D Cartesian configuration space. Thus $V_{at} = \frac{1}{2}\alpha\parallel \boldsymbol{\Upsilon} - \boldsymbol{\Upsilon}_d \parallel^2$, were $\boldsymbol{\Upsilon}_d = \mathbf{0}_{6\times1}$ is the desired destination of goal workspace. Then, $V_{at} = \frac{1}{2}\alpha\parallel \boldsymbol{\Upsilon} \parallel^2$ where α is a positive scaling factor and $\boldsymbol{\Upsilon}_j = [\mathbf{t}_j, (\mathbf{u}\theta)_j]_{j=0}^k$ is a parametrization of end-effector workspace. Thus the attractive potential force is:

$$\mathbf{F}_{at}(\boldsymbol{\Upsilon}) = -\vec{\nabla}V_{at\boldsymbol{\Upsilon}} = -\alpha\boldsymbol{\Upsilon}. \tag{2.31}$$

The role of the repulsive potential force $\mathbf{F}_{rp}(\boldsymbol{\Upsilon})$ is to push the robot away from the constraints such as obstacles. The desired repulsive potential force $\mathbf{F}_{rp}(\boldsymbol{\Upsilon}) = -\vec{\nabla}V_{rp}$ is the sum of two terms: the obstacle-avoidance-potential force $\mathbf{F}_{rp\mathcal{O}}(\boldsymbol{\Upsilon}) = -\vec{\nabla}V_{rp\mathcal{O}}$, and the visibility constraints of potential force $\mathbf{F}_{rp\mathcal{V}}(\boldsymbol{\Upsilon}) = -\vec{\nabla}V_{rp\mathcal{V}}$. The goal of the repulsive potential force is to push the robot's desired points away from the defined constraints.

As illustrated in Figure 2.11, a visibility constraint implies a potential barrier function denoted by $V_{rp\mathcal{V}}$ to push the robot to reach the goal state while remaining in the camera's field of view. A visibility constraint implies a potential barrier force to push the mobile robot to reach the goal configuration while remaining in the camera's field of view hence guarantees that robot stays in the visibility range of the overhead camera. We define the suitable repulsive potential function denoted by $V_{rp\mathcal{O}}$ in the image space to generate a trajectory avoiding any obstacle with an arbitrary shape. We assume that $V_{rp\mathcal{O}}$ is a continuous non-negative potential field and differentiable function whose value tends to infinity in desired point belonging to the obstacles. This repulsive potential field is called Force Inducing an Artificial Repulsion from the Surface of the obstacle (FIARS):

$$V_{rp\mathcal{O}}(\rho) = \begin{cases} 1/2\eta(\frac{1}{\rho} - \frac{1}{\rho_0})^2 & ,if\rho \leq \rho_0 \\ 0 & ,if\rho \geq \rho_0, \end{cases} \tag{2.32}$$

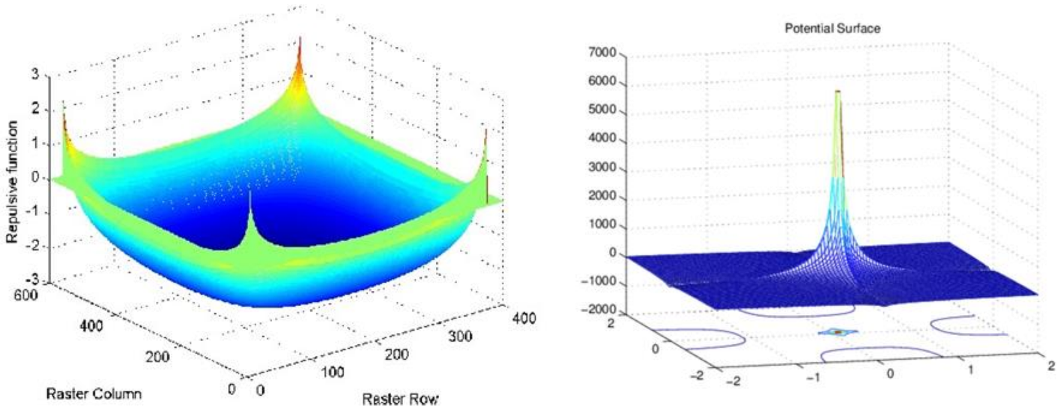

Figure 2.11: Mesh plot of repulsive potential function called FIRAS is used for obstacles which is defined in point (0,0) of desired potential surface, (right). Repulsive barrier function for camera's field of view constraint, (left)

where η is a positive scaling factor, and ρ is the shortest Euclidean distance between the robot and the obstacle surface, and ρ_0 is the limited distance of the repulsive potential field influence.

The total repulsive potential fields comprise the obstacle-avoidance and the visibility constraints repulsive potential fields.

$$\mathbf{F}_{rp}(\boldsymbol{\Upsilon}) = \mathbf{F}_{rp\mathcal{V}}(\boldsymbol{\Upsilon}) + \mathbf{F}_{rp\mathcal{O}}(\boldsymbol{\Upsilon}). \tag{2.33}$$

Each point of the robot can be subjected to the defined APF. The final repulsive potential function is the summation of all repulsive potential functions created by each obstacle within the measuring distance between the robot projection points and the specified obstacle border in the image space. The discrete time trajectory along the direction of the artificial potential force $\mathbf{F}(\boldsymbol{\Upsilon})$ is obtained via (2.29). Therefore, the discrete geometric path is performed as a sequence of k intermediate points that is avoiding the visibility constraints as well as the specified obstacles. The four 6×1 vectors of generated trajectory $\boldsymbol{\Upsilon}_j = [\mathbf{t}_j, (\mathbf{u}\theta)_j]_{j=0}^{k}$ determine the current obstacle-free path for the vertices of the moving robot.

The classic APF method is a straightforward method that does not require excessive computational power. However, the major problem in the real-time path planning using APF method is the local minimum issue, which can make a trap for a robot before reaching its goal location. However, by considering the entire path in global path planning the problem of being trapped in a local minimum is greatly reduced.

Figure 2.12 shows the generated path (positions and orientations) of the end-effector proposed in [**P3**], from initial to desired pose. In [**P2**], we consider the end-effector mounted camera is under the influence of defined APF which is sum of two terms including the attractive potential field and the repulsive potential field. The attractive potential field's role is to pull the end-effector toward the desired target pose and the repulsive potential field's role is to push the end-effector away from constraints such as obstacle. In [**P3**], we consider that the camera is fixed over the robot workspace and the 6 DOF end-effector is under the influence of the defined APF. In [**P4**] – [**P6**], the mobile robots are under the influence of the defined APF to pull the mobile robots toward the desired pose and push them away from constraints.

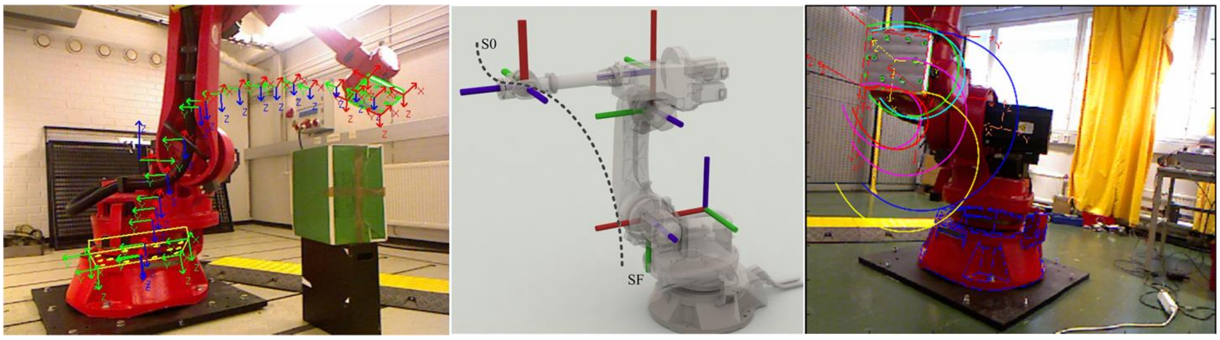

Figure 2.12: The generated path in [**P**3], guarantees that the robot end-effector remains in the camera's field of view during the operation task. This technique gives the operator a depth cue by visualizing the 6D generated path for the end-effector from initial to desired pose in the image space.

2.3.1 Image-based Path Planning

A survey of vision-based navigation and mapping with various aspects of the progress was done by DeSouza and Kak (2002). The image-based path planning algorithm straightforwardly selects a feasible path to an objective image while avoiding static obstacles and singular points synchronously. Path planning in image space for robust VS was introduced by Mezouar and Chaumette (2000). This technique consists of path planning from initial camera frame to desired camera frame while the camera is mounted on robot's end effector. This method increases the applicability of VS when initial and desired poses are distant.

Most of vision-based path planning methods use stereo vision systems. For instance Ude and Dillmann (1994) employed a stereo vision system and proposed a vision-based algorithm based on a CAD model of the object to be manipulated. This method employed the "teaching by showing " programming paradigm. At each measurement instant, a stereo image pair is taken and a list of straight line segments is extracted. This system allows the user to specify a desired trajectory by moving a fairly general object to be manipulated with his or her hand. Hosoda et al. (1995) proposed a trajectory generator based on the potential field method using a stereo system applied to obstacle avoidance. Paper by Hummel et al. (2006) deals with the path planning in image space for outdoor robots with the underlying probabilistic framework that allows reliable obstacle detection. In this method, different types of vision sensors such as laser range finders plus inertial navigation systems supply vehicle positioning data. Noborio and Nishino (2001) presented an approach for image-based path planning for investigating an objective image in a three or more dimensional joint space.

2.3.2 Global Path Planning

Path planning, sometimes called "motion planning," can be categorized into two main groups: local path planning and global path planning, see Figure 2.13. Local path planning is based on measured sensor information in uncertain environments in which the obstacles positions are not known. Global path planning is the process that uses prior information to allow an autonomous robot to find the optimized path to reach a desired position. This process has two main steps including gathering the available information into an effective and appropriate configuration space and then using a search algorithm to find the optimized path in that space based on the work space's predefined criteria. The first step in the planning process is to map the workspace into the configuration space C_{space} of the robot.

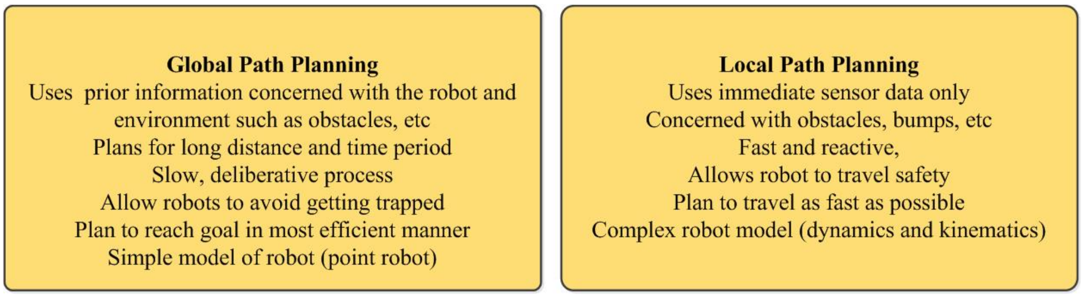

Figure 2.13: Global path planning versus local path planning for unmanned ground vehicles Giesbrecht (2004).

Configuration space is a multidimensional space intersected by a set of generalized coordinates that describe the position and orientation of a desired rigid object. C_{space} determines the position and orientation of a moving object represented by a single point. The obstacles can be represented by forbidden regions. The planning problem is then reduced to moving the point representing the robot configuration from an initial position to a desired position without countering any of the obstacle regions. The main drawback of global path planning method is that the global workspace must be known at the time of the path planning, while only local information is required for local path planning. However, the benefits of global path planning are more important than its disadvantages, especially in path planning problems neglecting uncertainty. As proposed by Warren (1989), by considering the whole generated path, the problem of robot becoming trapped by a local minimum is reduced significantly. This allows the method to be used for global path planning. The proposed algorithms are effective for mobile robot path planning problems involves sets of convex obstacles. Otherwise, the potential field may not be convex and local minima can trap the robot.

In [**P4**], we propose a new global path planning method for the omni-directional mobile robot with 4WS based on the defined APF. It consists of planning paths for mobile robot with a set of n points lying on the target in the image space. Collisions between the obstacles and the robot are avoided by a repulsive force between them that simplifies the negative gradient of the potential field. The generated path is always in the camera field of view and hence guarantees that robot stays in the visibility range of the overhead camera. Figure 2.14 shows the vision-based path coordination for three mobile robots with 4WS, presented in [**P**6]. We extend our previous work in global path planning method, to present the decoupled path coordination method based on a vision system. It provides the necessary information about obstacles as well as the mobile robot's position and orientation in the initial and desired poses. We can compute the geometrical traces for actual volume of mobile robots and their possible intersection region, even in a confined shared workspace.

2.3.3 Robots Trajectory Planning

Trajectory planning is one of the fundamental problems that determine a feasible motion that permits a mobile robot to move from initial state to final state in the presence of kinematic and dynamic constraints. Compared with human ability, a robot controller has to solve many problems to realize even simple motions in a workspace. Depending

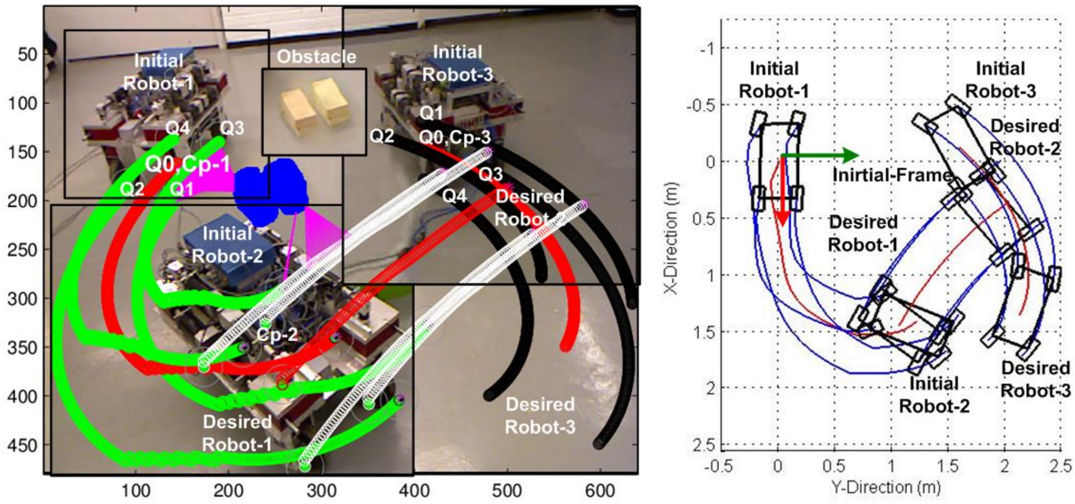

Figure 2.14: Generated vision-based individual paths in the image space (left) and the corresponding global path in the world coordinates (right), proposed in [**P**6] for three mobile robots with 4WS while avoiding two types of obstacles including: (1) recognized static obstacles in the image space (two bricks) and (2) image boundaries.

on prior environmental information and final planning results, most of the proposed trajectory planning methods can be divided into local and global methods. Local methods are specified by the local knowledge of the environment. At each displacement, the local method algorithm determines the existence or absence of collisions to modify the trajectory. However, global methods are based on knowledge of the entire workspace. Looking at the vast literature concerned with both local and global methods, a number of researchers have proposed different techniques for different conditions to solve trajectory planning for manipulators and mobile robots.

2.3.3.1 Manipulators

The purpose of many manipulator applications, such as welding and spray painting, is to plan a sequence of motions that the manipulator must traverse with its end-effector along a desired path while whole robot's body avoids any collision with obstacles. Motion of the robotic manipulator in accessible static environment by considering all the kinematic constraints may be easily planned. However, the manipulator dynamics are highly non-linear, see for instance, the method proposed by M. Aref et al. (2014). Therefore, the manipulator obstacle avoidance while considering the full robot dynamic model is very difficult.

In the case of manipulators with many joints, the motion limitation of the all individual joints and actuators for velocity, acceleration, and jerk constraints must be considered. General types of constraints for conventional trajectory planning of manipulator are included in the system constraints imposed by the manipulator itself and constraints determined by the task and environment. The generated trajectory can be specified in joint space or in Cartesian space. In Cartesian space, the pose of the end-effector is known only in initial and desired pose. Cartesian trajectories make it easy to specify the motion of the manipulator's end-effector. However, joint motion is obtained via the manipulator Jacobian. Actually, while dealing with trajectory planning approaches, a desired joint trajectory is specified in terms of a set of via-points between the initial and the end point to satisfy the limits for the joint velocities, acceleration, jerks and so forth.

Various assumptions or simplifications according to the complexity of kinematics and dynamics of the robot manipulator were proposed in Thompson and Patel (1987), and Pfeiffer and Johanni (1987). Many researchers have separated manipulator trajectory planning problems into several smaller tractable sub-problems with different constraints. To name a few of these sub-problem based methods: the collision-free path planning methods proposed by Yang and Meng (2000), the time-optimal velocity planning methods along a specified path proposed by Cao et al. (1994), and the vision-based path planning proposed by Mezouar and Chaumette (2002).

2.3.3.2 Mobile Robots

Trajectory planning for mobile robots is only one aspect of the global navigation problem to direct an autonomous mobile robot from a current pose to the desired pose based on the prior global map. Basic mobile robot navigation task can be divided into the following main sub-tasks Kunchev et al. (2006):

- Environment perception and modeling.
- Collision-free path planning.
- Planning the trajectory.

Many trajectory planning methods with different approaches were solved only by modeling the robot's environment, such as the visibility graph presented by Everett et al. (2002), the voronoi diagram proposed by Brandt and Algazi (1992), and the cell decomposition method proposed by Pas (1989). Only very few trajectory planning methods for mobile robots concentrate on geometric 3D models of the mobile robot and its interaction with the environment for instance, Munoz et al. (1994). From this point of view, most often path planning methods model the robot using only one point that moves with constant velocity to execute the path perfectly. However, this one point robot model assumption is not realistic for many applications.

Mobile robots have been used in various applications, such as search and rescue, exploration, hazard detection and analysis. They can be divided into two categories based on their motion generation capabilities: non-holonomic and holonomic mobile robots. As illustrated in Figure 2.15, there are many types on non-holonomic mobile robots, such as three-wheeled differential drive, car-like vehicles and omni-directional mobile robot.

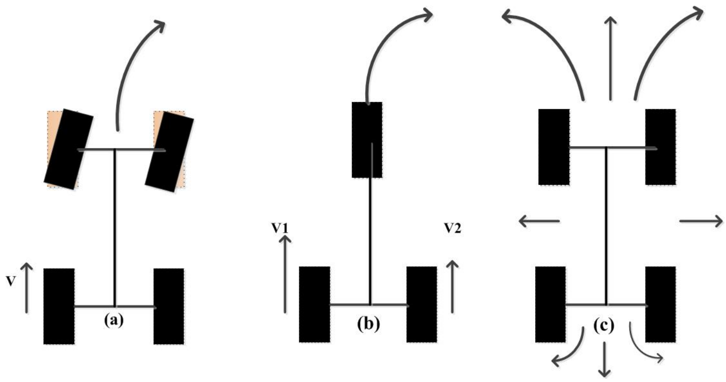

Figure 2.15: Car-like vehicle (a), three-wheeled differential drive (b), and Omni-directional mobile robot (c).

A car-like robot is a typical non-holonomic robot that can only move forward and backward in a direction tangent to its main axis. A three-wheeled differential drive mobile robot has two independently driven wheels. A four wheels omni-directional mobile robot is capable of achieving 4 DOF motions by driving 4 independent actuators, see for instance, Campion and Chung (2008). Omni-directional mobile robots have the ability to move concurrently and independently in rotation and movement in the plane with high maneuverability to realize any arbitrary independent set of linear and angular velocities, see Figure 2.16.

This means their translational and rotational motions can be controlled independently at any time. Therefore, omni-directional mobile robots can move sideways and forward in addition to rotating. The great benefit of them is that they are able to navigate tight quarters and have few constraints in regard to path planning. Both path and trajectory planning are very difficult task, especially when the robot dynamic constraints are considered and in the presence of moving obstacles. There are many approaches to solve this problem, each are based on a different set of assumptions.

In conventional trajectory planning methods, complex equations must be solved to generate a smooth and continuous path for mobile robots that satisfies an arbitrary number of constraints involving position, heading, and/or curvature, and linear and angular velocities. Research on mobile robots with independently steerable-wheels has drawn much attention in recent years, for example the methods proposed by Chen et al. (2012), Jung et al. (2011), and Oftadeh et al. (2013b). Several approaches have been proposed for trajectory planning in relatively static environments, such as the methods proposed by Chen et al. (2012), Jung et al. (2011), Moore and Flann (1999), and Kalmár-Nagy et al. (2004). Roughly speaking all of these approaches utilizes two main steps: first, a geometrical collision-free path is built, and then secondly, a feedback control system is incorporated to determine the heading angle and track the path. The major drawback of these methods is their relative complexity in the kinematic and dynamic models and the need for designing separate controllers for the robot's position and orientation Samani et al. (2004). The main objective in these approaches is the collision avoidance. Other criteria, such as time optimality, which was introduced by Moore and Flann (1999), are most often neglected. In the methods that deal with optimal control criteria, such as the method proposed by Kalmár-Nagy et al. (2004), the focus is on position control, and the heading is neglected.

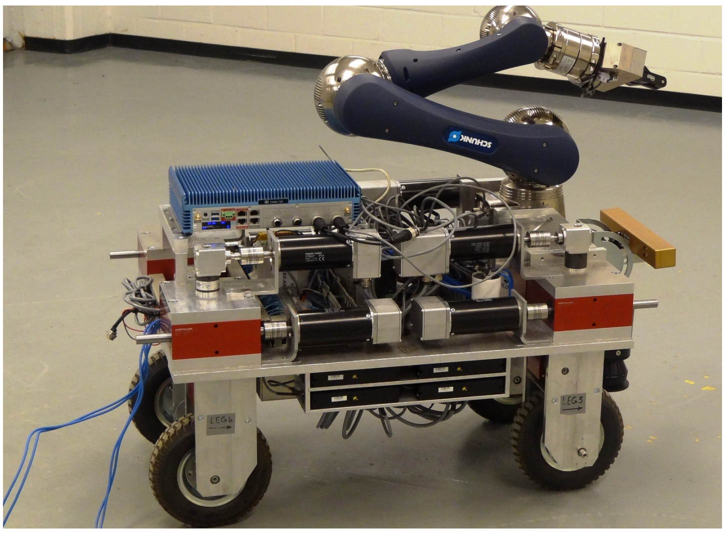

Figure 2.16: Non-holonomic omni-directional mobile robot with four independently steering wheels, called *i*Moro Oftadeh et al. (2013a).

The wheel's rotation and translation planning are the main factors in trajectory planning for mobile robots with steerable wheels as presented by Wang and Qi (2001). Another important factor in the success of these methods is synchronization of the wheels to avoid slippage and misalignment in movement. Trajectory planning for a 4WS vehicle presented by Wang and Qi (2001) develops a trajectory planning algorithm based on a kinematic model of the mobile robot. This research consists of two main parts including the rotation planning and the translation planning for a mobile robot with 4WS. The orientation of a mobile robot with 4WS is not specified uniquely when moving along a specified path. Therefore, the robot heading angle as one constraint is needed to fully determine the orientation of the mobile robot.

The complexity of path and trajectory planning depends on the environment assumptions, presence of static or dynamic obstacles, and the geometric and dynamic robot models used to represent the robot motion. The defined initial assumption and basic concepts were introduced by Munoz et al. (1994) to describe the kinematics model of the mobile robot. However, these initial assumptions are not realistic for many applications. The method proposed by Munoz et al. (1994) considers the mobile robot as only one point and use a sequence of splines to generate a path that includes way-points. Continuous curved paths provide good conditions to be followed by omni-directional mobile robots. The splines contained time information, so that the robot's desired velocity can be limited depending on the hardware used.

In this thesis, we consider the main following assumptions and concepts in vision-based trajectory planning using geometric kinematic modeling of omni-directional mobile robots:

1. The whole geometric shape of the mobile robot is considered including the wheels and robot center points.
2. The mobile robot motion with 4WS can be divided only into translation and rotation components.
3. The motion of each robot wheel can be expressed only in translation and rotation.
4. The linear and angular velocities of the mobile robot are planned with maximum allowable velocities.

In [**P5**], based on above assumption, we proposed a vision-based method to generate the synchronized trajectories for all wheels of mobile robot with 4WS. Figure 2.17 shows midpoints of the generated synchronized trajectories for the all steering wheels of mobile robots in the world coordinates. These generated synchronized trajectories simplify the complexity of the mobile robot kinematic model to obtain desired kinematic variables for planning maximum allowable linear and angular velocities. As illustrated in Figure 2.17, we assume that the inertial-frame $\mathbf{U}\{\hat{\mathbf{X}}, \hat{\mathbf{Y}}\}$ is attached to the fixed starting point Q. Unsynchronized wheels can result in slippage and misalignment in translation and rotation movement as well as several other issues, Schwesinger et al. (2012). To overcome these problems, the points on the generated trajectories for all wheels have to form a unique Instantaneous Center of Rotation (ICR) which defined by Clavien et al. (2010). We can obtain ICR to plan maximum allowable velocities for each wheel so that at least one of the actuators works at the maximum allowable velocities without becoming saturated.

In [**P6**], we address the problem of coordinating the multiple mobile robots with 4WS in the shared workspace. They must avoid mutual collisions to reach their independent goals,

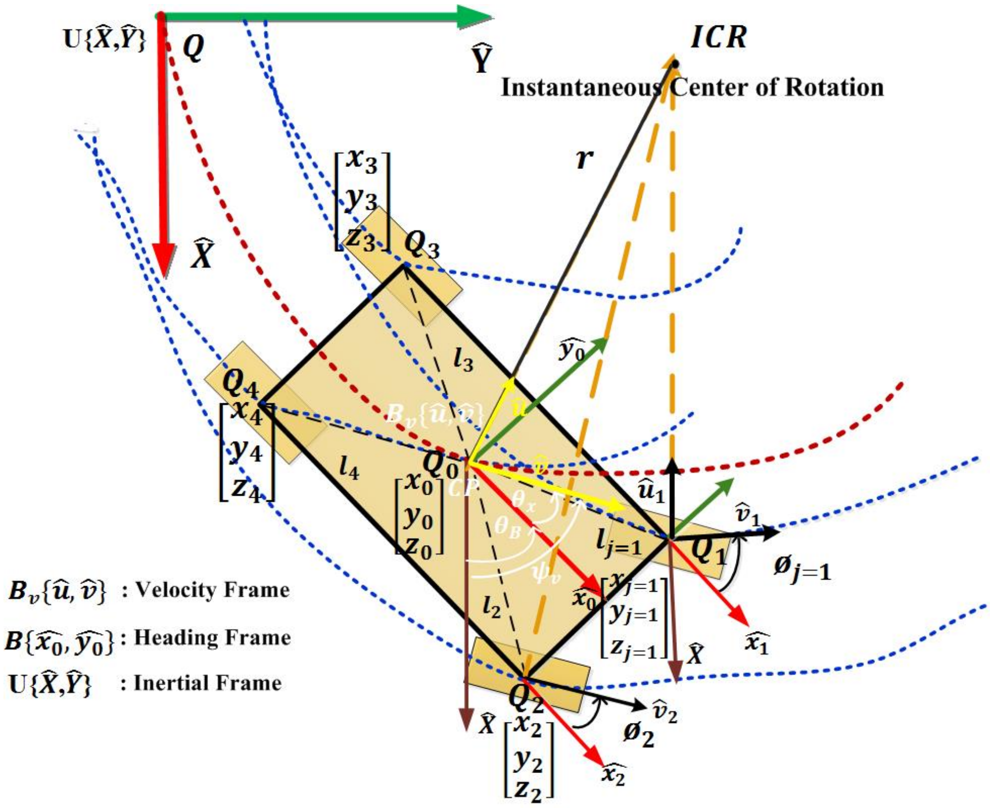

Figure 2.17: Generated synchronized trajectories via vision-based method presented in [**P**5], for the all steering wheels $Q_0, Q_1, ..., Q_4$, simplify the complexity of kinematic model. To plan the robot velocity, the instantaneous center of rotation (ICR) can be estimated using at least two synchronized generated trajectories of the wheels on omni-directional mobile robot.

so that the generated paths are always in the camera field of view, guaranteeing that the robots stay in the visibility range of the overhead camera. A mobile robot with 4WS is a type of nonholonomic mobile robot with omnidirectional steering wheels that are able to move along any direction, simultaneously attaining desired orientation. Trajectory coordination determines the robots position and velocity along a given generated path while avoiding stationary obstacles as well as mutual collision.

To coordinate the motion of multiple mobile robots along their generated obstacle-free path, it is necessary to compute the intersection region that can be achieved using individual traces that may intersect in the shared configuration time-space. The geometrical traces determine not only the intersection region between the multiple mobile robots but also the edges of the mobile robot wheels that may intersect with another moving mobile robot, in time-space configuration. Therefore we are able to estimate the time of collision with desired velocities in the generated paths to avoid it. Then, the generated geometrical traces for robots that move forward in time-space are employed to assign the priorities of the moving mobile robots in sequence.

Based on the generated trajectories that determine the possible intersection regions, the mobile robot that must move to avoid only the static obstacles has higher priority. Furthermore, the mobile robot that must move to avoid both the stationary and higher priority mobile robot has lower priority. The lower priority mobile robots switch to the halt mode to avoid the intersection boundaries and wait for the higher priority mobile robots to pass. The generated trajectories and corresponding traces with respect to the robot inertial-frame in time-space configuration determine the minimum time of the halting mode for lower priority mobile robots. Time delays are inserted to resolve potential collisions. This process is continued until all of the mobile robots with 4WS reach their individual goals.

2.4 Summary of the State-of-the-Art

In this section, we summarize the state-of-the-art that is explained in previous sections. As explained in [**P1**] – [**P6**], the camera calibration parameters in presence of radial lens distortion are necessary for pose estimation and obtaining the visual servoing variables. We employ the CAD-based recognition method to obtain pose of the desired object with only one CCD camera. The vision-based 2D-3D pose estimation method is used to calculate the desired pose mainly by matching the re-projection 3D model of the object and its corresponding features in the image.

Autonomous robot collision avoidance requires an accurate separation of obstacles from the background. In [**P3**] – [**P6**], we use color information as our primary cue to segment the obstacles using the HSV color filter method which proposed by Sural et al. (2002). These types of methods basically consist of detecting pixels that are different in appearance on the ground and then classifying them as obstacles.

A combination of the PBVS and the IBVS concepts are used to obtain the necessary visual servoing variables such as end-effector velocity screw and Jacobian matrix to generate desired path proposed in [**P2**] – [**P6**]. The required repulsive potential fields and forces can be calculated using these visual servoing concepts. These concepts define the variation of robot coordinates to the variation of generated trajectory with respect to the fixed overhead camera. For instance, in [**P2**], we consider the 6 DOF end-effector equipped with a CCD camera is under the influence of the defined APF. The attractive potential field's role is to pull the end-effector toward the desired target pose and the repulsive potential field's role is to push the end-effector away from the defined constraints. Path planning for mobile robot, is designing the geometric consideration way from point A to point B. However, trajectory planning is problem of determining both a path and velocity function for a robot. The vision-based trajectory planning method presented in [**P5**]-[**P6**], generate the synchronized paths and trajectories for all wheels of Omni-directional mobile robots with 4WS. The entire generated paths are always in the camera field of view and hence guarantees that robots stay in the visibility range of the overhead camera. These synchronized trajectories simplify the complexity of the kinematic model for such mobile robot to easily estimate the necessary variables of kinematic models. Then we plan maximum allowable driving and steering velocities.

In [**P6**], we have developed the vision-based path planning method to present the path coordination method for multiple mobile robots with 4WS to avoid mutual collisions, so that the generated paths are always in the visibility range of the overhead camera. The main contribution of the proposed vision-based method is coordinating the trajectories for multiple mobile robots to avoid intersection boundaries that are obtained by generated geometrical traces in real world coordinates.

3 Summary of Publications

This chapter provides the summary of publications [**P1**] – [**P6**].

3.1 Real-time markerless Augmented Reality for Remote Handling system in Bad Viewing Conditions

Due to expected levels of nuclear radiation inside the ITER vacuum vessel, ITER Divertor scheduled maintenance requires development of various RH operations. For RH maintenance operations a radiation tolerant vision system is required. In ITER, manipulators have arms with high degree of freedom that lead to complex kinematic models. Manipulator WHMAN is installed on top of a Cassette Multifunctional Mover (CMM) to carry out a wide variety of RH operations inside a ITER Divertor such as cutting, bending and welding of pipes, locking and unlocking of cassettes, etc.

Publication [**P1**] addresses the problem of RH in hazardous and inaccessible to human environments. In this paper, we extend markerless AR for RH applications in ITER Divertor Cassette Locking system as a case study. AR refers to the combination of virtual objects and real world environments, so that operator can experience a realistic illusion to explore the real world environments. Several technologies and approaches of AR implementations are available today. These technologies can be divided in two basic groups including marker-based systems and markerless systems. The latter is based on markerless solutions, meaning that markerless pose trackers rely on natural object features which are visible in the tracking environments.

In this research, we employ a markerless AR technique using a template-based matching algorithm to produce a virtual environment superposed on visible or occluded user's view to track and detect the manipulator end-effector in near real-time during the RH operation tasks. The main motivation of this work is to help the operator in RH operations to tackle the lack of sufficient visual feedback due to the limited number of on-site cameras, the not optimized poses of the cameras, failures, poor viewing angles, and etc.

The proposed method enables the operator to estimate and display the 3D position and 3D orientation of the end-effector with respect to the camera frame. The fixed camera frame coordinates can be transformed to the manipulator body frame coordinates. Therefore, the rotation angle and translation of the manipulator can be obtained with respect to the manipulator base frame. It was shown that the proposed AR-RH can assist the operations required in ITER workspace in near real-time. The method proposed in this journal paper is validated in real RH scene.

3.2 New Scheme for Image Space Path Planning Incorporating CAD-based Recognition Methods for Visual Servoing

Path planning in image space has been studied especially in order to generate the feasible trajectory for the VS controllers. The main idea of image-based path planning introduced by Mezouar and Chaumette (2002), is to derive a practical paths for image features based on IBVS while taking into account variety of constraints imposed by the image itself and the physical environments.

In many practical cases especially in cluttered workspace, extracting the image features is not always robust enough and the target features are not to be occluded by the obstacles, robot's body or the target object itself. One of the main challenges of VS is maintaining continuous visibility for target tracking inside the camera's field of view. In image-based path planning for VS, the initial and desired poses in 3D Cartesian space should be visible. Several approaches in 2D-3D pose estimation category have been proposed. Most of the proposed methods extract the object features in the image to match them with corresponding points of model to circumvent the geometric search space and estimate the object pose. These methods are computationally efficient and quite easy to realize. However, since the tracking process is based on matching the edges in the image space by local search algorithms, it can rapidly fail in face of large initial pose differences. Furthermore, the pose estimation loses its robustness in the presence of cluttered background that often happens in practical applications.

The CAD-based recognition method via monocular image is a popular method to recognize the object and estimate its pose with known geometry. Also this method is robust to noise, partial occlusion, clutter and lighting change. In [**P1**], we developed this method as a markerless AR for assistive RH task. The lack of aided trajectory as a feedback motivated us to solve this challenge via path planning in image space for markerless manipulator tasks.

In [**P2**], we propose an image-based path planning method for markerless 3D targets to generate consistent 6D path for end-effector from the initial to desired pose while the camera is mounted on the robot's end effector. The generated path remains inside the image boundaries during the robot operation task. In this research, we integrate a 3D CAD-based recognition method with an image-based path planning approach to compose a new path planning scheme that graciously enhances the manipulation performance while the camera is mounted on the robot's end effector. By utilizing this method, we able to generate desired path for 3D target even some parts of the object are occluded by external occlusions or by itself.

This approach takes into account both position and orientation of the end-effector with respect to the camera frame between initial and desired pose such that the 3D target stays in the camera's field of view. The generated 3D path can be transformed to the end-effector center coordinates. Therefore, the end-effector can follow the generated 6D path in the world coordinates.

3.3 Assistive Obstacle-Free Path Planning in the Image Space for Teleoperation Tasks Using Monocular Camera

One of the most challenging tasks in the ITER for the precise RH task is the Cassette-Locking Divertor. The intricacy in such RH tasks often mandates the use of high degree of freedom manipulators in very constraint space environment. Thus, the use of the camera-in-hand for such RH task can be very challenging. Another feature that adds to the complexity of the problem is the high degree of freedom manipulator that is installed on top of a mobile platform in order to reach the required workspace. Therefore, the desired pose to be reached by the end-effector is partially unknown with respect to the robot-base frame.

The essential subsystems of a RH system include the operator, the master arm, and the communication link between these two. The operator is always in the control loop as an active controller to manage the performance of teleoperation tasks. In conventional and precise RH tasks, a teleoperator must exercise extreme care especially in the presence of obstacles and practical restrictions, such as limited number of on-site cameras, poor depth perception, display-control misalignment, collisions, and inaccessible operation tasks. The main motivation in this research is to increase the level of autonomy of system for such complex RH operations in hazardous environments.

To increase the level of autonomy, in publication [**P1**], we proposed a method to tackle the lack of sufficient visual feedback for the human operator which is due to the limited number of on-site cameras. However, the proposed method in [**P1**] is not able to guide the operator to find the obstacle-free path to reach the desired pose. In [**P2**], we enhanced the manipulation performance while the camera is mounted on robot's end effector.

In order to increase the level of autonomy and system performance, in paper [**P3**], we extend our previous approaches to present an obstacle-free path planning method for manipulators while the camera is fixed above the robot workspace. In this case study, we consider the 6D manipulator mounted on top of the mobile platform. Since the relative desired pose of the end-effector with respect to the robot-base may change in each round of the RH task. Therefore, the final pose of the end-effector is partially unknown with respect to the robot-base.

The proposed path planning method is relatively simple to implement and accurate enough to provide the generated path (positions and orientations) for the end-effector from initial to desired pose by utilizing visual cues. This method guarantees that the robot end-effector and the generated path remain in the camera's field of view during the operation task. Furthermore, this technique gives the operator a depth cue by visualizing the 6D generated pose of the end-effector in the 2D image frame.

Displaying the color-cue coordinates frames of the 6D generated path enables the operator with powerful and direct depth cue as well as the correct position and orientation of the end-effector even when the moving object are partially occluded. Displaying the generated 6D path has potential to reduce operator stress and increases the system performance. The experimental results verify the capability of the proposed method to assist the operator in RH tasks.

3.4 Global Path Planning with Obstacle Avoidance for Omni-directional Mobile Robots Using Overhead Camera

The path planning algorithm is one of the most important functions in mobile robot navigation. The modeling or mapping the static or dynamic environment is another required task. The path planning component is divided into two categories including global path planning and local path planning. Global path planning methods are based on the prior information of the robot workspace. However, local path planning methods are based on measured sensory information in uncertain and unknown environments.

In [**P4**], we extend our previous work to present a new method in global path planning for an omni-directional mobile robots with steerable wheels utilizing an overhead camera. In this case, the robot motion can be interpreted as the motion of the recognized points of the mobile robots that are projected in the image space. A predefined map using the grabbed images of the robot workspace are necessary to determine the 3D environments into 2D image space.

Based on the VS concepts, we assume the projection points of the mobile robot in the image space are under the influence of the APF to move the mobile robot toward the goal without any collisions. To solve the problem, we fuse the image-based path planning method using VS concepts with APF to generate an obstacle-free path with respect to the camera frame. The proposed algorithm is able to find the optimal and safe path while the projection points of the generated path are entirely in the image boundaries. Two types of obstacles are avoided including static objects, which are recognized in the image space, and the image boundaries, which act as an obstacle that keep the generated path always within the camera's field of view. The generated path in the image space can be transformed to the mobile robot inertial frame in the start point, to generate a global and safe obstacle-free path in the world coordinates with respect to the robot inertial frame.

The major problem in the real-time path planning using the APF method is the local minimum issue, which can trap a robot before it reaches its goal location. However, by considering the entire off-line path, the local minimum problem is reduced and allowing the method to be used for global path planning. Experiment results presented the efficiency of the proposed method for the 4WS omni-directional mobile robot called iMoro.

3.5 Vision-based Trajectory Planning for Four Wheel Independently Steered Mobile Robots with Maximum allowable Velocities

Publication [**P5**] addresses the problem of vision-based trajectory planning for mobile robots with 4WS in the environments that are hazardous and inaccessible to humans. An extensive example of such hazardous environments in large-scale environments is CERN LHC 27 km long tunnel, that requires high mobility and maneuverability while the camera is the only visual feedback. The use of mobile robots in such environments minimizes the danger of radiation exposure to humans. However, the robots themselves are also vulnerable to the radiation. Efficient time-optimal motion and trajectory planning algorithms in such environments are required to find a safe trajectory with maximum bounded velocities from a given starting configuration to a goal configuration.

The high maneuverability of omni-directional mobile robots with 4WS makes them suitable for inspection or transportation tasks in such confined environments in the presence of obstacles, where the robot must be kept in the camera's field of view. The main motivation of this work is to take the advantage of the proposed method for inspection tasks for 4WS mobile robots with high maneuverability in hazardous environments such as CERN LHC tunnel.

In this paper, we extend our previously proposed algorithm to present a novel method for generating synchronized trajectories for each wheel on mobile robots. This method defines the relation between the generated collision-free paths of the robot's wheels in the image space and its corresponding generated trajectories in the world coordinates. The vision-based algorithm generates synchronized trajectories that significantly simplify the complex kinematic model of 4WS mobile robots to obtain the necessary kinematic variables for velocities planning.

To plan the robot velocity, the 4WS mobile robot's ICR point in each trajectory midpoint is required. ICR is defined on the horizontal Cartesian plan with respect to the robot's center point with zero velocity while undergoing planar movement. By utilizing the synchronized trajectories, we can obtain the ICR to plan a maximum allowable driving and steering velocities for each robot wheel in such a way that at least one of the actuators works in a maximum allowable velocity without becoming saturated. The important advantage of this synchronized trajectory planning is to avoid wheel slippage and misalignment in translation and rotation movement.

3.6 Vision-Based Path Coordination for Multiple Mobile Robots with Four Steering Wheels Using an Overhead Camera

In publication [**P6**], we have further developed the method proposed in [**P5**] to present a new path-coordination method for multiple mobile robots with 4WS. We present the decoupled path coordination method for multiple mobile robots with 4WS in the shared workspace while avoiding mutual collisions as well as stationary obstacles. The generated paths are always in the camera's field of view, guaranteeing that the robots stay in range of the overhead calibrated CCD camera which is fixed above the robots workspace. Depending on the geometrical shape and size of the mobile robots' platforms and camera's field of view a limited number of mobile robots can move in the shared workspace.

These types of non-holonomic mobile robots with omni-directional steerable wheels are able to move along any direction and simultaneously attain the desired orientation. Such robots are more flexible than conventional holonomic mobile robots which make them suitable for moving in confined work spaces. Generating the corresponding paths for these types of mobile robots is more difficult as compared to conventional holonomic mobile robots.

In this paper, we have developed the vision-based path planning method to generate the synchronized obstacle-free trajectories for mobile robot's all wheels simultaneously. These generated synchronized trajectories determine the whole volume swept by each robot as its square shape added with the space swept by its wheels in the world coordinates where the heading angle is already computed. By utilizing this method, geometrical traces for all mobile robots can be obtained.

To coordinate the motion of multiple mobile robots along their generated obstacle-free paths, it is necessary to compute the intersection region that can be achieved using individual traces that may intersect in the shared configuration time-space. The mobile robot must move to avoid only the static obstacles has the higher priority. Furthermore, the mobile robot that must move to avoid both stationary objects and the higher priority mobile robots has lower priority. The lower priority mobile robots switch to the halt mode to avoid the intersection boundaries and wait for the higher priority mobile robots to pass. The generated trajectories and corresponding traces with respect to the robot's inertial-frame in time-configuration space determine the minimum time that the lower priority mobile robots spend in halt mode. Time delays are inserted to resolve potential collisions. This process is continued until all of the mobile robots have reached their individual goals.

We plan maximum allowable velocities for lower priority robots, taking into account the halting time required for higher priority robots to pass through the intersecting space. We continue this process for all mobile robots to reach their desired pose in the shared workspace. The main motivation of this work is to take the advantage of the proposed method for multiple mobile robots with 4WS to accomplish tasks, such as maintenance and inspection tasks in the confined workspace that are hazardous and inaccessible to humans.

4 Conclusion

This chapter presents the conclusions of this thesis. The main focus in this research is on vision-based methods for path planning and trajectory generation for high degree of freedom manipulators and mobile robots with independently steerable wheels. The following conclusions are based on the publications that are the major outcome of this research work.

Markerless Augmented Reality in RH Process: In [**P1**], we investigate the applications of markerless AR for RH by the end-effector in poor viewing angles. The proposed method enables the operator to estimate and display the 6D pose of the end-effector center coordinates. However the proposed method requires a training process and is not able to guide the operator to determine the safe whole path.

Visual Servoing Concepts in Path Planning: We investigate the vision-method to generate the obstacle-free path for high degree manipulator to reach the desired pose by utilizing the integration of VS concepts and APF methods. In [**P2**], VS concepts define the relationship between the moving robot in the real world coordinates and image space while the camera is mounted on robot's end-effector. In a manipulation task, we determine, how an end-effector equipped with camera reaches its 3D desired pose while remaining within the camera's field of view. In the next papers [**P3**, **P4**, **P5**, and **P6**], the focus is on new concepts in VS tasks that define the relationship between the robot movement in the real world coordinates and corresponding movement in the image space while the camera is fixed above the robot workspace.

Generating 6D Path and Providing its Visualization: In [**P3**] displaying the color-cue coordinates frames of the 6D generated path provides a powerful and direct depth cue for the operator as well as the position and orientation of the end-effector even while some parts of the moving object are occluded. Displaying the generated 6D path reduces operator stress and increases the system performance.

Global Path Planning: In [**P4**], we integrate the image-based path planning method with the obstacle avoidance approach to generate an obstacle-free path with respect to the robot's inertial frame while the mobile robot avoid two types of obstacles. The first type of obstacle is the static objects in the robot workspace which recognized in the image. The second type of obstacle is the image boundaries, which act as an obstacle that keeps the generated path within the camera's field of view.

Synchronized Trajectory Planning: In [**P5**], we plan the wheel's rotation and translation, which are the main factors in trajectory planning for omni-directional mobile robots with 4WS. We proposed a vision-based algorithm to plan synchronized trajectories for mobile robot's all wheels simultaneously.

Vision-based Velocities Planning: In [**P5**], we investigate how vision-based generated synchronized trajectories simplify the complexity of the mobile robot kinematic model to obtain the necessary kinematic variables for velocity planning. We plan maximum allowable steering and driving velocities for all wheels of the 4WS mobile robot. The steering and driving velocities of the robot's center-point are determined so that at least one of the actuator's velocities is at maximum bound.

Vision-based Decoupled Path Coordination: In [**P6**], we focus on path coordination of multiple mobile robots with steerable wheels. By utilizing the generated synchronized trajectories, the mobile robot geometrical traces can be obtained as the square shape of a mobile robot added with the space swept by its wheels in the world coordinates. To coordinate the motion of multiple mobile robots along their generated obstacle-free paths, it is necessary to compute the intersection region. This can be achieved using individual traces that may intersect in the shared configuration time-space.

Further Work: In this thesis, a vision-based trajectory planning method is presented for omni-directional mobile robots with 4WS in confined and limited workspace and presence of obstacles with visibility constraint. The generated synchronized trajectories simplify the complex kinematic model of non-holonomic mobile robot and plan maximum allowable steering and driving velocities so that at least one of the actuators velocities is at maximum allowable bound. In the future work, this method will be extended to present vision-based trajectory planning method for ordinary non-omni-directional mobile robot with more mechanical constraints. These type of constraints will be taken into account at the task planning level such that mobile robot avoids its joint-limits during performance. In this method the mobile robot configuration will be acceptable if each of its components is sufficiently far away from its corresponding joints limits. Therefore, the suitable potential field is necessary to tend to infinity as mobile robot gets closer to joints limit. In the future work, mobile robot will remain in the camera field of view and all axes will avoid their joints limits.

Bibliography

Beard, R. W. and McLain, T. W., "Multiple uav cooperative search under collision avoidance and limited range communication constraints," in *Decision and Control, 2003. Proceedings. 42nd IEEE Conference on*, vol. 1. IEEE, 2003, pp. 25–30.

Beer, J., Fisk, A. D., and Rogers, W. A., "Toward a framework for levels of robot autonomy in human-robot interaction," *Journal of Human-Robot Interaction*, vol. 3, no. 2, p. 74, 2014.

Bhattacharya, P. and Gavrilova, M. L., "Roadmap-based path planning-using the voronoi diagram for a clearance-based shortest path," *Robotics & Automation Magazine, IEEE*, vol. 15, no. 2, pp. 58–66, 2008.

Bradski, G. and Kaehler, A., *Learning OpenCV: Computer vision with the OpenCV library.* O'Reilly Media, Inc., 2008.

Brandt, J. W. and Algazi, V. R., "Continuous skeleton computation by voronoi diagram," *CVGIP: Image understanding*, vol. 55, no. 3, pp. 329–338, 1992.

Campion, G. and Chung, W., "Wheeled robots," in *Springer Handbook of Robotics.* Springer, 2008, pp. 391–410.

Cao, B., Doods, G., and Irwin, G. W., "Time-optimal and smooth constrained path planning for robot manipulators," in *Robotics and Automation, 1994. Proceedings., 1994 IEEE International Conference on.* IEEE, 1994, pp. 1853–1858.

Castaño, A. and Hutchinson, S., "Visual compliance: Task-directed visual servo control," *Robotics and Automation, IEEE Transactions on*, vol. 10, no. 3, pp. 334–342, 1994.

Cervera, E., Del Pobil, A. P., Berry, F., and Martinet, P., "Improving image-based visual servoing with three-dimensional features," *The International Journal of Robotics Research*, vol. 22, no. 10-11, pp. 821–839, 2003.

Chen, C., Qin, H., and Yin, Z., "Trajectory planning for omni-directional mobile robot based on bezier curve, trigonometric function and polynomial," in *Intelligent Robotics and Applications.* Springer, 2012, pp. 352–364.

Chintamani, K., Cao, A., Ellis, R. D., and Pandya, A. K., "Improved telemanipulator navigation during display-control misalignments using augmented reality cues," *Systems, Man and Cybernetics, Part A: Systems and Humans, IEEE Transactions on*, vol. 40, no. 1, pp. 29–39, 2010.

Clavien, L., Lauria, M., and Michaud, F., "Instantaneous centre of rotation estimation of an omnidirectional mobile robot," in *Robotics and Automation (ICRA), 2010 IEEE International Conference on.* IEEE, 2010, pp. 5435–5440.

Colito, J., "Autonomous mission planning and execution for unmanned surface vehicles in compliance with the marine rules of the road," Ph.D. dissertation, University of Washington, 2007.

Comport, A. I., Marchand, E., Pressigout, M., and Chaumette, F., "Real-time markerless tracking for augmented reality: the virtual visual servoing framework," *Visualization and Computer Graphics, IEEE Transactions on*, vol. 12, no. 4, pp. 615–628, 2006.

Corke, P. I. and Hutchinson, S. A., "A new hybrid image-based visual servo control scheme," in *Decision and Control, 2000. Proceedings of the 39th IEEE Conference on*, vol. 3. IEEE, 2000, pp. 2521–2526.

Dementhon, D. F. and Davis, L. S., "Model-based object pose in 25 lines of code," *International journal of computer vision*, vol. 15, no. 1-2, pp. 123–141, 1995.

DeSouza, G. N. and Kak, A. C., "Vision for mobile robot navigation: A survey," *Pattern Analysis and Machine Intelligence, IEEE Transactions on*, vol. 24, no. 2, pp. 237–267, 2002.

Eskandarian, A., *Handbook of intelligent vehicles.* Springer London, 2012.

Everett, P. B. H., Houle, S. P. F. M. E., Meijer, A. L. H., Rote, K. R. G., Whitesides, T. C. S. S., and Zelle, C., "A visibility representation for graphs in three dimensions," *Graph Algorithms and Applications I*, p. 103, 2002.

Fischler, M. A. and Bolles, R. C., "Random sample consensus: a paradigm for model fitting with applications to image analysis and automated cartography," *Communications of the ACM*, vol. 24, no. 6, pp. 381–395, 1981.

Giesbrecht, J., "Global path planning for unmanned ground vehicles," DTIC Document, Tech. Rep., 2004.

Gold, S., Rangarajan, A., Lu, C.-P., Pappu, S., and Mjolsness, E., "New algorithms for 2d and 3d point matching: Pose estimation and correspondence," *Pattern recognition*, vol. 31, no. 8, pp. 1019–1031, 1998.

Goldberg, A. V. and Harrelson, C., "Computing the shortest path: A search meets graph theory," in *Proceedings of the sixteenth annual ACM-SIAM symposium on Discrete algorithms.* Society for Industrial and Applied Mathematics, 2005, pp. 156–165.

Guzel, M. S. and Bicker, R., "Optical flow based system design for mobile robots," in *Robotics Automation and Mechatronics (RAM), 2010 IEEE Conference on.* IEEE, 2010, pp. 545–550.

Halcon, M. (2007) MVtec Software GMbH. [Online]. Available: http://www.halcon.com/halcon/hdevelop/hdevengine.html

Haralick, R. M., Joo, H., Lee, C.-N., Zhuang, X., Vaidya, V. G., and Kim, M. B., "Pose estimation from corresponding point data," *Systems, Man and Cybernetics, IEEE Transactions on*, vol. 19, no. 6, pp. 1426–1446, 1989.

Horaud, R., Dornaika, F., and Lamiroy, B., "Object pose: The link between weak perspective, paraperspective, and full perspective," *International Journal of Computer Vision*, vol. 22, no. 2, pp. 173–189, 1997.

Hosoda, K., Sakamoto, K., and Asada, M., "Trajectory generation for obstacle avoidance of uncalibrated stereo visual servoing without 3d reconstruction," in *Intelligent Robots and Systems 95.'Human Robot Interaction and Cooperative Robots', Proceedings. 1995 IEEE/RSJ International Conference on*, vol. 1. IEEE, 1995, pp. 29–34.

Hummel, B., Kammel, S., Dang, T., Duchow, C., and Stiller, C., "Vision-based path-planning in unstructured environments," in *Intelligent Vehicles Symposium, 2006 IEEE*. IEEE, 2006, pp. 176–181.

Ismail, A.-T., Sheta, A., and Al-Weshah, M., "A mobile robot path planning using genetic algorithm in static environment," *Journal of Computer Science*, vol. 4, no. 4, pp. 341–344, 2008.

Iwata, A., Kato, K., and Yamamoto, K., "The detective of the obstacle by using the new system called horizon view camera," *Proceeding of Asian Conference on Computer Vision*, vol. 1, pp. 235–240, 2002.

Jung, E.-j., Yi, B.-J., and Kim, W. K., "Motion planning algorithms of an omni-directional mobile robot with active caster wheels," *Intelligent Service Robotics*, vol. 4, no. 3, pp. 167–180, 2011.

Kala, R., Shukla, A., and Tiwari, R., "Robotic path planning in static environment using hierarchical multi-neuron heuristic search and probability based fitness," *Neurocomputing*, vol. 74, no. 14, pp. 2314–2335, 2011.

Kalmár-Nagy, T., D'Andrea, R., and Ganguly, P., "Near-optimal dynamic trajectory generation and control of an omnidirectional vehicle," *Robotics and Autonomous Systems*, vol. 46, no. 1, pp. 47–64, 2004.

Kato, H. and Billinghurst, M., "Marker tracking and hmd calibration for a video-based augmented reality conferencing system," in *Augmented Reality, 1999.(IWAR'99) Proceedings. 2nd IEEE and ACM International Workshop on*. IEEE, 1999, pp. 85–94.

Khatib, O., "Real-time obstacle avoidance for manipulators and mobile robots," *The international journal of robotics research*, vol. 5, no. 1, pp. 90–98, 1986.

Kuffner, J. J. and LaValle, S. M., "Rrt-connect: An efficient approach to single-query path planning," in *Robotics and Automation, 2000. Proceedings. ICRA'00. IEEE International Conference on*, vol. 2. IEEE, 2000, pp. 995–1001.

Kunchev, V., Jain, L., Ivancevic, V., and Finn, A., "Path planning and obstacle avoidance for autonomous mobile robots: A review," in *Knowledge-Based Intelligent Information and Engineering Systems*. Springer, 2006, pp. 537–544.

Kyrki, V., Kragic, D., and Christensen, H. I., "Measurement errors in visual servoing," *Robotics and Autonomous Systems*, vol. 54, no. 10, pp. 815–827, 2006.

Lingelbach, F., "Path planning using probabilistic cell decomposition," in *Robotics and Automation, 2004. Proceedings. ICRA'04. 2004 IEEE International Conference on*, vol. 1. IEEE, 2004, pp. 467–472.

Liu, S., Sun, D., and Zhu, C., "Coordinated motion planning for multiple mobile robots along designed paths with formation requirement," *Mechatronics, IEEE/ASME Transactions on*, vol. 16, no. 6, pp. 1021–1031, 2011.

Lucas, B. D., Kanade, T. *et al.*, "An iterative image registration technique with an application to stereo vision." in *International Joint Conference on Artificial Intelligence*, 1981.

Lumelsky, V. J. and Harinarayan, K., "Decentralized motion planning for multiple mobile robots: The cocktail party model," in *Robot colonies*. Springer, 1997, pp. 121–135.

M. Aref, Mohammad, M., Ghabcheloo, R., and Mattila, J., "A macro-micro controller for pallet picking by an articulated-frame-steering hydraulic mobile machine," in *Robotics and Automation (ICRA), 2014 IEEE International Conference on*. IEEE, 2014, pp. 6816–6822.

Malis, E., Chaumette, F., and Boudet, S., "21/2d visual servoing," *Robotics and Automation, IEEE Transactions on*, vol. 15, no. 2, pp. 238–250, 1999.

Mezouar, Y. and Chaumette, F., "Path planning in image space for robust visual servoing," in *Robotics and Automation, 2000. Proceedings. ICRA'00. IEEE International Conference on*, vol. 3. IEEE, 2000, pp. 2759–2764.

———, "Design and tracking of desirable trajectories in the image space by integrating mechanical and visibility constraints," in *Robotics and Automation, 2001. Proceedings 2001 ICRA. IEEE International Conference on*, vol. 1. IEEE, 2001, pp. 731–736.

———, "Path planning for robust image-based control," *Robotics and Automation, IEEE Transactions On*, vol. 18, no. 4, pp. 534–549, 2002.

Moore, K. L. and Flann, N. S., "Hierarchical task decomposition approach to path planning and control for an omni-directional autonomous mobile robot," in *Intelligent Control/Intelligent Systems and Semiotics, 1999. Proceedings of the 1999 IEEE International Symposium on*. IEEE, 1999, pp. 302–307.

Morel, G., Liebezeit, T., Szewczyk, J., Boudet, S., and Pot, J., "Explicit incorporation of 2d constraints in vision based control of robot manipulators," in *Experimental Robotics VI*. Springer, 2000, pp. 99–108.

Munoz, V., Ollero, A., Prado, M., and Simon, A., "Mobile robot trajectory planning with dynamic and kinematic constraints," in *Robotics and Automation, 1994. Proceedings., 1994 IEEE International Conference on*. IEEE, 1994, pp. 2802–2807.

Noborio, H. and Nishino, Y., "Image-based path-planning algorithm on the joint space," in *Robotics and Automation, 2001. Proceedings 2001 ICRA. IEEE International Conference on*, vol. 2. IEEE, 2001, pp. 1180–1187.

Oftadeh, R., Aref, M. M., Ghabcheloo, R., and Mattila, J., "Bounded-velocity motion control of four wheel steered mobile robots," in *Advanced Intelligent Mechatronics (AIM), 2013 IEEE/ASME International Conference on*. IEEE, 2013, pp. 255–260.

Oftadeh, R., Ghabcheloo, R., and Mattila, J., "A novel time optimal path following controller with bounded velocities for mobile robots with independently steerable wheels," in *Intelligent Robots and Systems (IROS), 2013 IEEE/RSJ International Conference on*. IEEE, 2013, pp. 4845–4851.

Parker, L. E., "Path planning and motion coordination in multiple mobile robot teams," *Encyclopedia of Complexity and System Science. Springer, Heidelberg*, 2009.

Pas, J., "Uniform p-adic cell decomposition and local zeta functions," *J. reine angew. Math*, vol. 399, pp. 137–172, 1989.

Pfeiffer, F. and Johanni, R., "A concept for manipulator trajectory planning," *Robotics and Automation, IEEE Journal of*, vol. 3, no. 2, pp. 115–123, 1987.

Samani, A., Abdollahi, A., Ostadi, H., and Rad, S. Z., "Design and development of a comprehensive omni directional soccer player robot," *International Journal of Advanced Robotic Systems*, vol. 1, no. 3, pp. 191–200, 2004.

Sanchez, G. and Latombe, J.-C., "Using a prm planner to compare centralized and decoupled planning for multi-robot systems," in *Robotics and Automation, 2002. Proceedings. ICRA'02. IEEE International Conference on*, vol. 2. IEEE, 2002, pp. 2112–2119.

Schwesinger, U., Pradalier, C., and Siegwart, R., "A novel approach for steering wheel synchronization with velocity/acceleration limits and mechanical constraints," in *Intelligent Robots and Systems (IROS), 2012 IEEE/RSJ International Conference on*. IEEE, 2012, pp. 5360–5366.

Siméon, T., Leroy, S., and Lauumond, J.-P., "Path coordination for multiple mobile robots: A resolution-complete algorithm," *Robotics and Automation, IEEE Transactions on*, vol. 18, no. 1, pp. 42–49, 2002.

Simo-Serra, E., Quattoni, A., Torras, C., and Moreno-Noguer, F., "A joint model for 2d and 3d pose estimation from a single image," in *Computer Vision and Pattern Recognition (CVPR), 2013 IEEE Conference on*. IEEE, 2013, pp. 3634–3641.

Steger, C., Ulrich, M., and Wiedemann, C., "Machine vision algorithms and applications," *Qinghua university publication*, vol. 355, pp. 1–3, 2008.

Stentz, A. *et al.*, "The focussed d^* algorithm for real-time replanning," in *IJCAI (Vol.95,pp.1652-1659)*, 1995.

Sural, S., Qian, G., and Pramanik, S., "Segmentation and histogram generation using the hsv color space for image retrieval," in *Image Processing. 2002. Proceedings. 2002 International Conference on*, vol. 2. IEEE, 2002, pp. II–589.

Thomas, J., "Empirical evaluation of a machine vision system for random bin picking application," Fachhochschule Bonn-Rhein-Sieg University of Applied Sciences, 8 2008, master Thesis.

Thompson, S. E. and Patel, R. V., "Formulation of joint trajectories for industrial robots using b-splines," *Industrial Electronics, IEEE Transactions on*, no. 2, pp. 192–199, 1987.

Turk, M. A. and Marra, M., "Color road segmentation and video obstacle detection," in *Cambridge Symposium_Intelligent Robotics Systems*. International Society for Optics and Photonics, 1987, pp. 136–142.

Ude, A. and Dillmann, R., *Vision-based robot path planning*. Springer, 1994.

Ulrich, I. and Nourbakhsh, I., "Appearance-based obstacle detection with monocular color vision," in *Innovative Applications of Artificial Intelligence Conference (IAAI)*, 2000.

Ulrich, M., Wiedemann, C., and Steger, C., "Cad-based recognition of 3d objects in monocular images," in *International Conference on Robotics and Automation*, vol. 1191, 2009, p. 1198.

Vale, A. and Ribeiro, I., "Mobile robot navigation for remote handling operations in iter," in *III Workshop de Robotica: Robotica Experimental*, 2011.

Velagic, J., Lacevic, B., and Perunicic, B., "A 3-level autonomous mobile robot navigation system designed by using reasoning/search approaches," *Robotics and Autonomous Systems*, vol. 54, no. 12, pp. 989–1004, 2006.

Wang, D. and Qi, F., "Trajectory planning for a four-wheel-steering vehicle," in *International Conference on Robotics and Automatio (ICRA), 2001 IEEE/RSJ International Conference on.* IEEE, 2001, pp. 3320–3325.

Warren, C. W., "Global path planning using artificial potential fields," in *Robotics and Automation, 1989. Proceedings., 1989 IEEE International Conference on.* IEEE, 1989, pp. 316–321.

Yanco, H. A. and Drury, J. L., "Classifying human-robot interaction: an updated taxonomy." in *Systems, Man and Cybernetics, 2004. Proceedings. SMC (3). IEEE International Conference on.* IEEE, 2004, pp. 2841–2846.

Yang, S. X. and Meng, M., "Real-time collision-free path planning of robot manipulators using neural network approaches," *Autonomous Robots*, vol. 9, no. 1, pp. 27–39, 2000.

Publications

Publication 1

Real-time markerless Augmented Reality for Remote Handling system in bad viewing conditions

by

Z. Ziaei, A. Hahto, J. Mattila, M. Siuko, and L. Semeraro,

International Journal of Fusion Engineering and Design, vol 86, no. 9

pp: 2033-2038, Jan 2011.

Fusion Engineering and Design 86 (2011) 2033–2038

Contents lists available at ScienceDirect

Fusion Engineering and Design

journal homepage: www.elsevier.com/locate/fusengdes

Real-time markerless Augmented Reality for Remote Handling system in bad viewing conditions

Z. Ziaei[a,*], A. Hahto[a], J. Mattila[a], M. Siuko[b], L. Semeraro[c]

[a] Department of Intelligent Hydraulics and Automation (IHA), Tampere University of Technology, P.O. Box 589, FI-33720 Tampere, Finland
[b] VTT Technical Research Centre of Finland, P.O. Box 1300, FI-33101 Tampere, Finland
[c] F4E, Fusion for Energy, Torres Diagonal Litoral B3, Josep Pla 2, 08019 Barcelona, Spain

ARTICLE INFO

Article history:
Available online 18 February 2011

Keywords:
Augmented Reality
Remote Handling
Template based matching
CAD-model
Position
Orientation

ABSTRACT

Remote Handling (RH) in harsh environments usually has to tackle the lack of sufficient visual feedback for the human operator due to the limited number of on-site cameras, the not optimized position of the cameras, the poor viewing angles, occlusion, failure, etc. Augmented Reality (AR) enables the user to perceive virtual computer-generated objects in a real scene. The most common goals usually include visibility enhancement and provision of extra information, such as positional data of various objects. The proposed AR system first recognizes and locates the markerless object by using a template based matching algorithm, and then augments the virtual model on top of the recognized item. The tracking algorithm is exploited for locating the object in a continuous sequence of frames. Conceptually, the template is found by computing the similarity between the template and the image frame, for all the relevant template poses (rotation and translation). As a case study, AR interface was displaying measured orientation and transformation of the Water Hydraulic Manipulator (WHMAN) Divertor preloading tool, in near real-time tracking. The bad viewing condition implies on the case when the view angle is such that the interesting features of the object are not in the field of view. The method in this paper was validated in concrete operational context at DTP2. The developed method proved to deliver robust positional and orientation information while augmenting and tracking the moving tool object.

1. Introduction

Due to expected levels of radiation inside the ITER vacuum vessel, emitted from activated components and many parts of the machine, ITER Divertor scheduled maintenance requires development of various remotely operable devices and equipment. For RH maintenance operations a radiation tolerant vision system is required. The Water Hydraulic Manipulator (WHMAN) at Divertor Test Platform 2 (DTP2) laboratory is a manipulator arm designed and manufactured in Tampere University of Technology, Department of Intelligent Hydraulic and Automation (IHA). WHMAN is installed on top of the Cassette Multifunctional Mover (CMM), to carry out wide variety of RH operations inside the ITER Divertor, such as cutting, bending and welding of pipes, locking and unlocking of cassettes, etc., during the installation and removal of cassettes [1].

The objective of the research presented in this paper is to study ways to help the WHMAN operator to perform his/her RH tasks in more safe and more efficient manner in bad viewing conditions of ITER. AR techniques have been considered as user aiding tool in teleoperation systems. Recent studies show that AR has the potential to improve teleoperation and RH efficiency [2,7,8].

In other words, AR features should be considered for increasing operator's perception during ongoing task strategies, by improving the information quality of the video feedback. In addition, techniques based on visualizing the 3D graphic knowledge of real scene, via AR, are some of the solutions in poor viewing conditions. The AR display method has been recently used in many manipulation systems [6–8]. A case study is presented in this paper, implementing a markerless AR interface display and providing WHMAN operator three orientation angles of the WHMAN tool WHjack, in near real-time (about 0.3 s) on a normal computer.

2. Remote Handling and Augmented Reality

A successful RH process is defined with its ability to specify and integrate together the appropriate technologies, organizational and management activities. Monitoring and controlling RH environment is provided by an integrated supervisory control and data acquisition system, including computer-generated models of the scene and equipment of control systems. AR systems merge computer-generated graphics with a view of the

* Corresponding author. Tel.: +358 0404192019; fax: +358 3 3115 2240.
E-mail address: zahra.ziaei@tut.fi (Z. Ziaei).

0920-3796/$ – see front matter © 2011 Elsevier B.V. All rights reserved.
doi:10.1016/j.fusengdes.2010.12.082

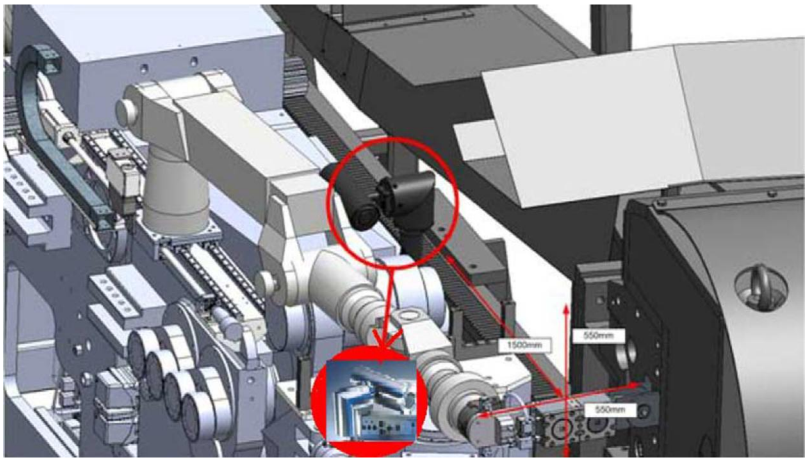

Fig. 1. Feasible system camera location in DTP2 laboratory.

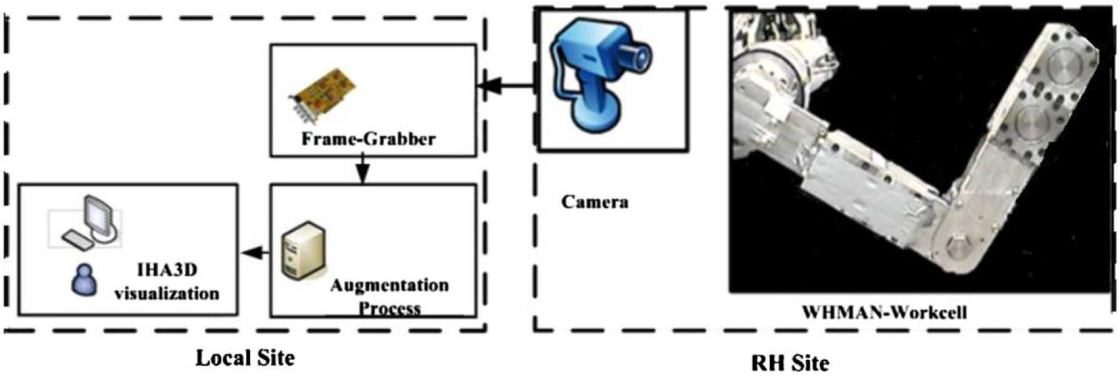

Fig. 2. Scheme of the system.

real physical world. Ideally, the graphics should be perfectly calibrated with the world physical reality. Perfect registration requires the accurate knowledge of the physical world and the spatial relationships between the world, the display and the viewer. However, in many real world situations, the available information is not accurate enough to support perfect registration [2]. An AR system acts an approach to create the superposition of additional scene data into the video stream of a real scene, in order to help the RH operator to perform his/her task efficiency and safety.

3. Description

In the following, we will describe the components of online markerless AR system in ITER-RH scenario which provides 3D position tracking in complex and unprepared RH scene, based on the template matching algorithm. Fig. 1 shows the feasible camera location with bad viewing condition in ITER-RH mock-up scene. In our experiment we suffer from bad view angle conditions. Furthermore, in 3D problems, limited number of on-site cameras (for our case only one camera) is another source of bad viewing.

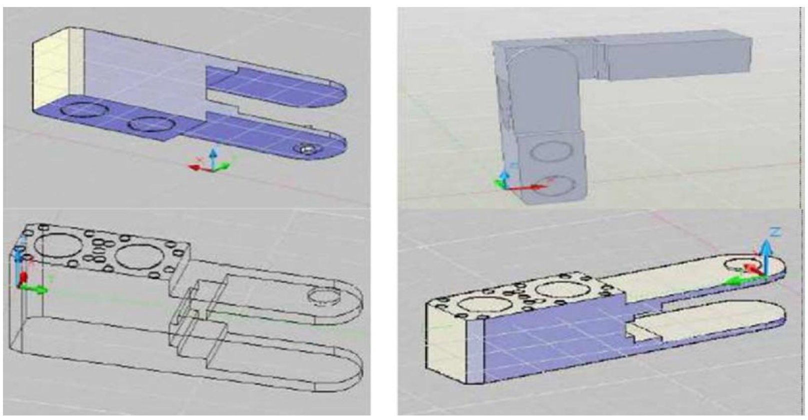

Fig. 3. 3D-CAD models of WHjack.

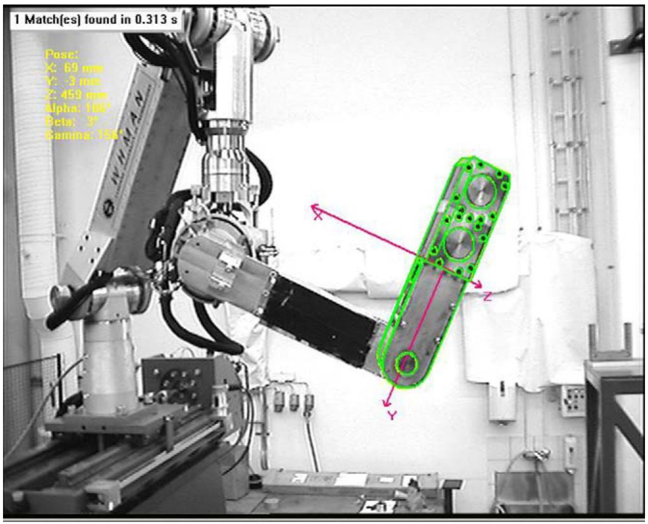

Fig. 4. Markerless augmentation process in the video stream.

3.1. Scheme of the system

The scheme of the AR system in RH environment is illustrated in Fig. 2. It is composed by two main parts: the RH site and, the local site including the augmentation and visualization subsystems. The local site equipments are directly accessible by the operator in a real scenario. In the opposite, RH-site equipments are probably out of touch because of radiation or other hazardous conditions. The operation of the WHMAN was done according to the planned tasks in RH-ITER and interaction capabilities based on AR together with 3D visualization software designed in IHA (IHA3D). The capture system consisted of one camera in feasible location, connected to frame-grabber.

The following are the major steps to capture WHjack position and orientation in RH site using augmented reality:

1. Camera Calibration; it defines the relationship between the real world and camera image coordinates. The pinhole camera establishes the mathematical relationship between central projections of 3D object plane to 2D image plane. The internal camera parameters define pixel coordinates of image point, in respect to coordinates in camera reference frame [3,6].
2. Creation a 3D CAD-model of WHjack; it was done with AutoCAD R12 (see Fig. 3).
3. Training process for tracking the WHjack-3D model; in order to create the matching correctly, the interior camera parameters used by the process must be passed as an input. The 3D shape model is generated by computing different views of the 3D object model, within an user-specified pose range. The CAD-model dimension scale is fitted to the real object with the user input manually [3,6].

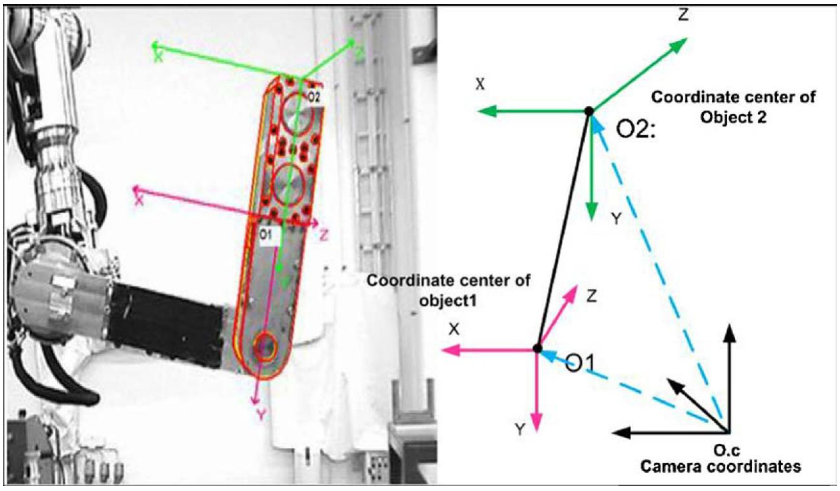

Fig. 5. Length measurement using two-augmentation processes.

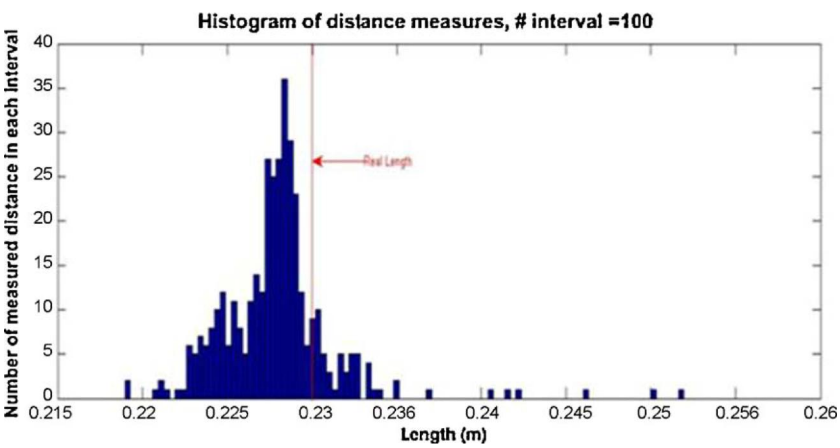

Fig. 6. Histogram of measured length date via AR.

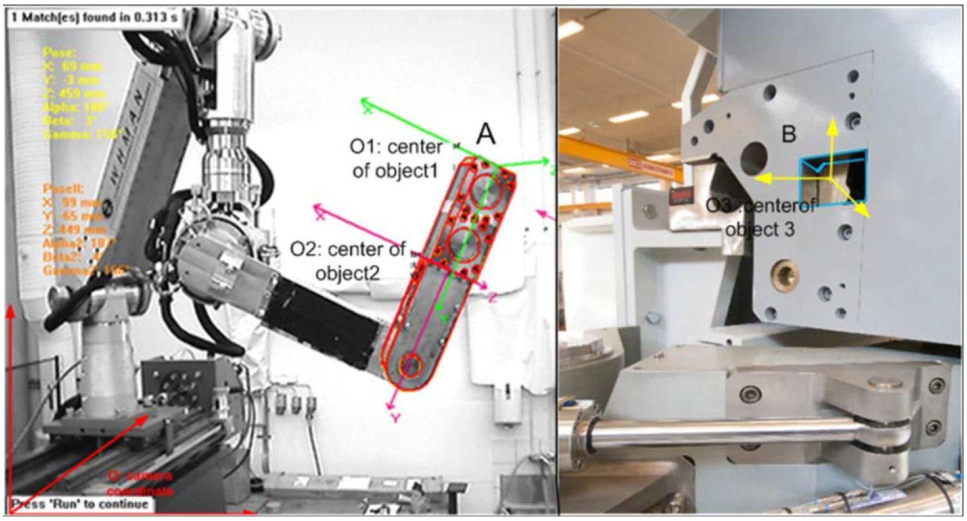

Fig. 7. Ongoing and future work (WHjack insertion).

4. Tracking and visualization of WHjack-3D model; the program uses template-based matching algorithm to find the 3D pose of WHjack exhibiting a six degrees of freedom motion view, from which the pose is subsequently refined and returned [3,4,6].
5. Projection and augmentation of WHjack-3D model; this step determines the edges of a 3D object model into the image coordinate system and augments the 3D object model to the frame in video stream, by projecting the shape model and the pose of the match [3,6].

3.2. Template based matching algorithm

One of the most popular methods to extract useful information from an image is the template based matching approach [4]. The tracking of a certain feature or target over time is based on the comparison of the content of each image with a sample template. Template matching algorithm can be found useful for several purposes. It can be used to detect the presence, or absence, of the object and to distinguish between different types of objects [4]. Use of Halcon library fulfils shape-based matching algorithm requirements, to find out the desired object based on a 3D model-template and to locate it with sub-pixel accuracy [3,4]. The behavior of light reflections during the AR depends on the illumination conditions. The useful information about the real illumination condition of ITER-RH environment has not been produced sufficiently [5].

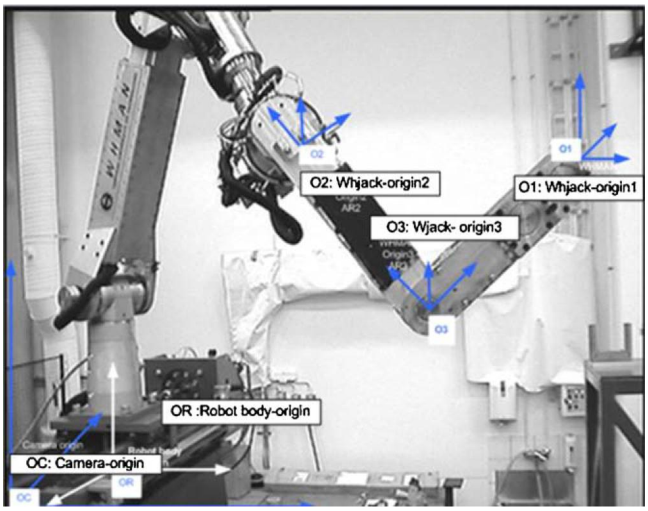

Fig. 8. Ongoing and future work (WHjack control).

4. Results

The coordinates of the 3D object model are given in the 3D world coordinates system. First, they are transformed into the camera coordinate system using the given pose and second, these coordinates are projected into the image coordinate system based on the interior camera parameters. The interior camera parameters describe the projection characteristics of the camera and the pose describes the position and orientation of the world coordinate system, with respect to the camera coordinate system [3].

The markerless AR user interface enables the augmentation of our desired markerless object. It enables us to project the coordinate system of the 3D object model and to display the parameters of the found pose in a video stream (see Fig. 4). The output display projects the coordinate axis to the image and shows the pose, including position (x, y, z) and orientation (α, β, γ) at the projected reference point consequently. The typical maximum time of tracking and finding the best match is 0.3 s. This setup presents a robust framework for 3D CAD-model based tracking of complex objects in unstructured environments.

During the AR process, the gravity center of CAD-model is used to measure the length between camera coordinate center and gravity center of the CAD-model. Depending on our objectives, the pose of the gravity center can be changed in the CAD-model creation steps.

Two parallel augmentation processes are used to measure the desired length between these two gravity centers, but it takes some more time than one-augmentation. Each instance is capable for tracking position and orientation using the given 3D-model of the desired object. Fig. 5 shows the length measurement application using two augmentation processes. Points O1 and O2 are the gravity centers of two augmented CAD-models in a real video stream. The real length measured in this experiment was 230 mm. The lengths via AR process were measured with transformation and slight-rotation and the distance between camera and WHjack was about 1500 mm. The histogram of measured length via AR process from 450 frames shows the distribution of measurements which is almost Gaussian (see Fig. 6). The mean value and real value are expected to be the same if and only if the measurement noise is zero-mean. Here the mean value (μ) is 227 mm and standard deviation (STD) is 3.4 mm and the normalized STD

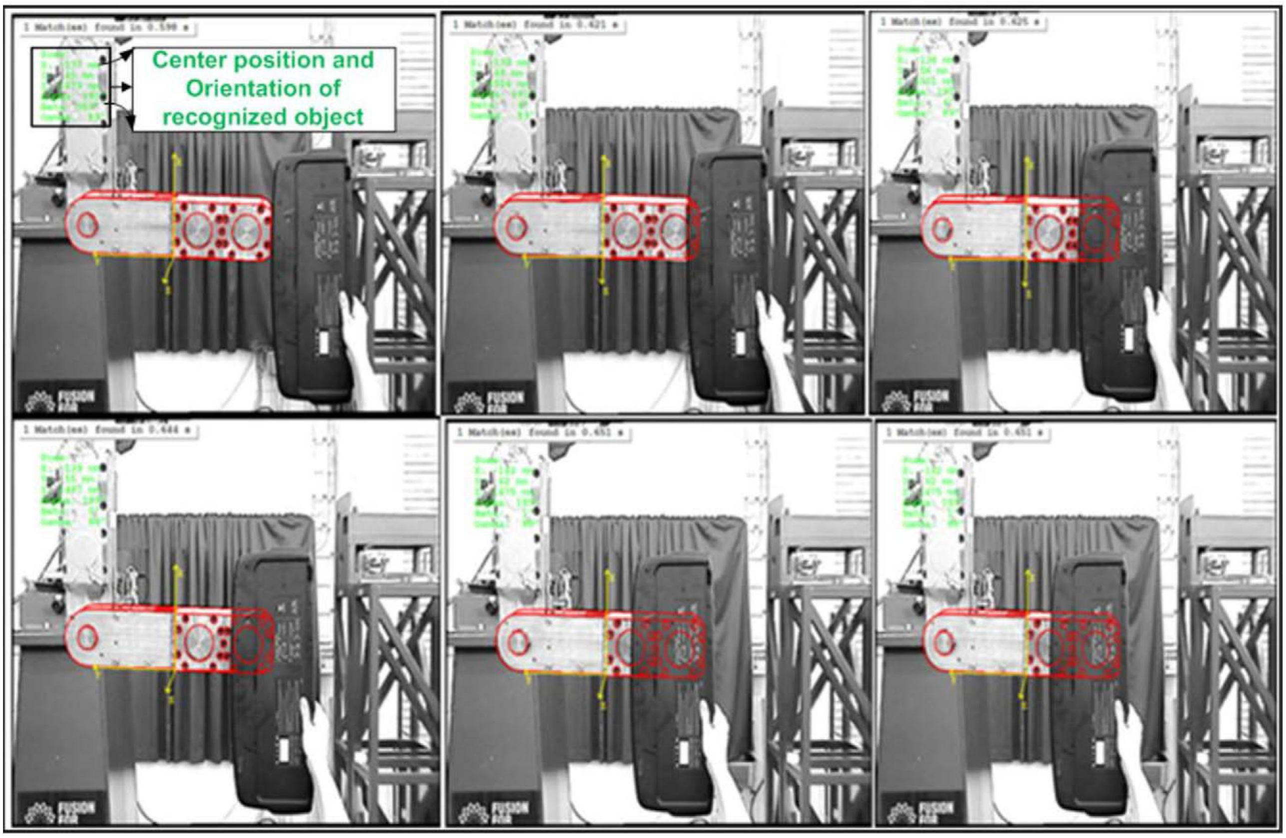

Fig. 9. AR via (5–40%) occluded views of WHjack.

is 0.0149% which implies robustness to transformation and slight rotation.

Current markerless AR gives extra information about the transformation and orientation of the object. In training step, we can teach the AR program to find the WHjack in different position and different orientations. Then, by using the already existing camera calibration data, position and orientation of WHjack can be determined reasonably.

5. Ongoing and future work

AR in ITER-RH can help the operator to control the motion of WHjack. The ongoing objectives for the case study (WHjack) are as follows:

5.1. WHjack Insertion

The first future goal is the WHjack insertion using markerless AR system includes the following proposed steps (Fig. 7):

1. Recognize and locate both markerless object 1 (WHjack) and object 2 (Slot), using template based matching algorithm in AR process.
2. Determine and display the location and orientation of the objects in three-dimensional workspace.
3. Immediate AR feedback can assist the operator for controlling actions of the system in near real-time.

5.2. WHjack control

The next future goal related the ITER project is to use the markerless AR for specifying the rotation and transformation as an immediate feedback to control WHjack motion (see Fig. 8). The proposed steps include:

1. Markerless AR gives position (x, y, z) and orientation (α, β, γ) of augmented WHjack-models. The orientations and rotations are defined in respect to the camera coordinate center that was calibrated via calibration process.
2. The fixed camera origin will be transformed to the fixed manipulator body origin.
3. The rotation angle of an object, in respect to the camera origin, will be translated to the rotation angle in respect to the manipulator body origin. The translated rotation as an AR redundant information can assist the operator directly.

5.3. Occlusion error

A significant visual cue for understanding the spatial relationship of objects in a RH scene is to correct the occlusion of object from user's viewpoint. This occlusion problem can be solved on condition that the model of 3D object is given.

Another future goal of the AR in RH is to find the object in images even if it is occluded, disturbed, or some part of the object is missed (see Fig. 9).

6. Conclusion

We have briefly introduced a markerless augmented reality application applied in the ITER project.

We successfully developed markerless AR interface in a RH-ITER mock-up environment, using template based matching algorithm to assist the operator as a visual feedback. The performance of the AR-RH system depends on hardware equipment (camera, illumination, etc.) as well as the software procedures (calibration method, matching algorithm) utilized for implementing the system. The AR process produced a virtual environment being superimposed on visible or occluded user's view.

The superimposed 3D CAD-model additionally specified the measured values of orientation and transformation of markerless WHjack, in near real-time tracking. The pose (position and orientation) of augmented 3D CAD-model was consequently displayed in the user's view. It was shown the AR-RH can assist the operator to remotely handle the equipment needed in ITER mock-up environment. The methods in this paper were validated in real RH scene and proven to be robust enough to rotation of object.

Acknowledgements

This work was carried out under the Grant F4E-2008-GRT-MS-RH-01 of the European Joint Undertaking for ITER and the Development of Fusion Energy (Fusion for Energy) and financial support of TEKES, which are greatly acknowledged. The views and opinions expressed herein do not necessary reflect those of Fusion for Energy or European Commission. Fusion for Energy is not liable for the use which might be made of the information in this publication.

References

[1] Remote Operation and Virtual Reality, ROViR. Available at: http://www.hermia.fi/rovir/in_english/rovir/dtp2/equipment/ (cited 4/5/2010).
[2] A. Kheddar, E.S. Neo, R. Tadakuma, K. Yokio, Enhanced teleoperation through virtual reality techniques Springer Tracts in Advanced Robotics: Advances in Telerobotics, vol. 31, 2007, pp. 139–159.
[3] Halcon Reference Manual. Available at: http://www.mvtec.com/download/reference/hdevelop/table_of_contents.html (cited 5/2010).
[4] C. Steger, M. Ulrich, C. Wiedemann, Machine Vision Algorithms and Applications, Wiley-VCH, 2002.
[5] R. King, D. Hamilton, Augmented virtualised reality applications and benefits in remote handling, Fusion Engineering and Design 84 (2009) 1055–1057.
[6] Z. Ziaei, Online markerless augmented reality in remote handling system, MSc Thesis, Department of IHA, Tampere University of Technology, 2010.
[7] M.V. Noyes, T.B. Sheridan, A novel predictor for telemanipulation through a time delays, in: Proceeding of the 20th Annual Conference on Manual Control, NASA Ames Research Center, Moffet Field, CA, 1984.
[8] R. Azuma, Y. Baillot, R. Behringer, S. Feiner, S. Julier, B. MacIntyre, Recent advances in augmented reality, IEEE Computer Graphics and Applications 21 (November/December (6)) (2001) 34–47.

Publication 2

New Scheme for Image Space Path Planning Incorporating CAD-Based Recognition Methods for Visual Servoing

by

Z. Ziaei, R. Oftadeh, and J. Mattila,

Proceeding of the IEEE International Conference on Robotics, Automation and Mechatronics, 2013 (RAM 2013), Manila, Philippines,

November 12-14, 2013, pp. 212-217.

Publication 3

Assistive Obstacle-Free Path Planning in the Image Space for Teleoperation Tasks Using Monocular Camera

by

Z. Ziaei, R. Oftadeh, and J. Mattila,

Proceeding of the IEEE International Conference on System Theory, Control and Computing, 2014 (ICSTCC 2014), Sinaia, Romania,

October 17-19, 2014, pp. 838-844.

Publication 4

Global Path Planning with Obstacle Avoidance for Omnidirectional Mobile Robots Using Overhead Camera

by

Z. Ziaei, R. Oftadeh, and J. Mattila,

Proceeding of the IEEE International Conference on Mechatronics and Automation, 2014 (ICMA 2014), Tianjin, China,

August 2-5, 2014, pp. 697-704.

This paper was nominated by IEEE ICMA 2014 Program Committee and Award Committee as a Best Paper Finalists in IEEE International Conference on Mechatronics and Automation

Publication 5

Vision-Based Trajectories Planning for Four Wheels Independently Steered Mobile Robots with Maximum Allowable Velocities

by

Z. Ziaei, R. Oftadeh, and J. Mattila,

Proceeding of the 16th Annual Conference on Towards Autonomous Robotic System, England, 2015 (TAROS 2015), Liverpool, England,

September 8-10, 2015, Springer, Vol. 9287, pp. 303-309.

Vision-Based Trajectories Planning for Four Wheels Independently Steered Mobile Robots with Maximum Allowable Velocities

Zahra Ziaei(✉), Reza Oftadeh, and Jouni Mattila

Department of Intelligent Hydraulics and Automation (IHA), Tampere University of Technology, Tampere, Finland
{zahra.ziaei,reza.oftadeh}@tut.fi

Abstract. In this paper, we extend our previous work to introduce a novel vision-based trajectories planning method for four-wheel-steered mobile robots. Relying only on the overhead camera and by utilizing artificial potential fields and visual servoing concepts, we simultaneously, generate the synchronized trajectories for all wheels in the world coordinates with sufficient number of trajectories midpoints. The synchronized trajectories are used to provide the robot's kinematic variables and robot-instantaneous-center of rotation to reduce the complexity of the robot kinematic model. Therefore, we plan maximum allowable velocities for all wheels so that at least one of the actuators is always working at maximum velocity. Experiment results are presented to illustrate the efficiency of the proposed method for four-wheel-steered mobile robot called *i*Moro.

Keywords: Vision-based · Trajectories planning · Steering velocity planning · Driving velocity planning

1 Introduction

Industrial and scientific applications of mobile robots are continuously growing particularly under accessibility considerations such as inspection and manipulation in environments that are inaccessible to human [1]. An extensive example of such hazardous and out-of-reach environments in large-scale scientific infrastructures is CERN[1] with a 27-km LHC[2] tunnel, that requires high mobility and maneuverability. While the use of mobile robots in such environments minimizes the danger of radiation exposure to human, the robots themselves are vulnerable to the radiation. Therefore efficient time-optimal motion and trajectory planning algorithms are required to find a safe trajectory with maximum bounded velocities from a given start configuration to a goal configuration. The main motivation of this work is to take advantage of the proposed method for inspection and manipulation tasks for four-wheel-steered (4WS) mobile robots with high maneuverability in confined and out-of-reach work spaces such as CERN tunnel.

[1] The European Organization for Nuclear Research.

[2] Large Hadron Collider.

C. Dixon and K. Tuyls (Eds.): TAROS 2015, LNAI 9287, pp. 303–309, 2015.
DOI: 10.1007/978-3-319-22416-9_34

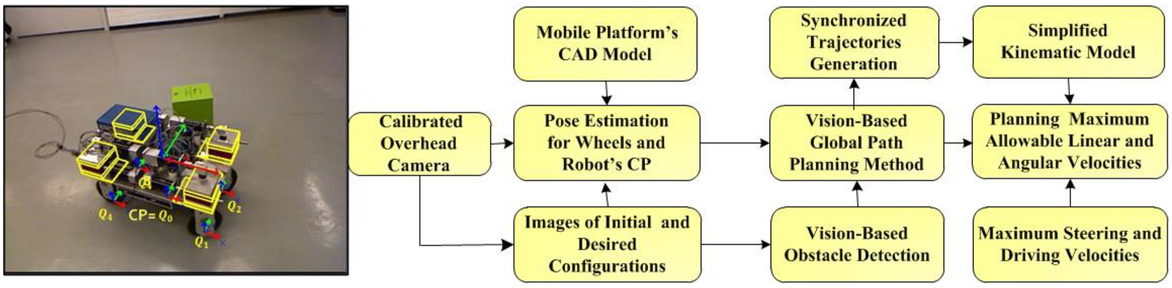

Fig. 1. Four wheels and robot's center point (CP) mapped in the ground are denoted by $\{Q_0, Q_1, ..., Q_4\}$ in the image space (right). System architecture of proposed vision-based trajectory planning for mobile robot with 4WS (left).

2 Vision-Based Trajectories Planning

In this paper, we present the vision-based method for generating the synchronized trajectories for all wheels of mobile robots with 4WS, to plan maximum allowable velocities so that at least one of the actuators is always working at maximum velocities. A mobile robot with 4WS is a type of the non-holonomic mobile robots with omni-directional steering wheels that are able to move along any direction simultaneously and attaining desired orientation. Such robots are more flexible than ordinary mobile robots which make them suitable for confined workspace such as manipulation task in camera field of view.

Figure 1 provides an overview of desired system architecture and the image space that determine the levels of proposed trajectories generation method. Unlike the conventional trajectory planning that consider the mobile robot as only one point, we consider 4WS mobile robot with its center-point (CP) plus the wheels CP with the same rotation and different positions, (see Fig. 1). CAD-based pose estimation method is used to recognize and estimate the position and orientation of the desired robot's points in the image space [2]. Approach for image-based obstacle segmentation method which explained in [2] are used to extract color features of the obstacle from the background.

In this paper, we defines the relationship between the motion of a mobile robot with 4WS, in the image space and in the world coordinates by utilizing the Artificial potential field (APF) integrated with visual servoing concepts, while the overhead camera is fixed. Inertial potential force is obtained by $\mathbf{F}(\boldsymbol{\Upsilon}) = \mathbf{F}_{at}(\boldsymbol{\Upsilon}) + \mathbf{F}_{rp}(\boldsymbol{\Upsilon})$, where attractive force $\mathbf{F}_{at}(\Upsilon)$ and repulsive force $\mathbf{F}_{rp}(\boldsymbol{\Upsilon})$ induced by proposed potential fields. The desired discrete-time trajectories for $\{Q_0, Q_1, ..., Q_4\}$ along the direction of 6×1 pose vector $\boldsymbol{\Upsilon}$ are obtained by the transition equation which generate trajectory midpoints for all desired points, simultaneously. A desired path along the direction of the artificial potential force is calculated via following equation [2]:

$$\boldsymbol{\Upsilon}_{k+1} = \boldsymbol{\Upsilon}_k + \epsilon_k \frac{\mathbf{F}(\boldsymbol{\Upsilon}_k)}{\| \mathbf{F}(\boldsymbol{\Upsilon}_k) \|}, \quad (1)$$

where k is an index that increases during the generation of a trajectory, and ϵ_k is a positive scaling factor. We allow the algorithm to generate sufficient number of midpoints by increasing ϵ_k. Then, we can easily transform each k-th generated trajectory to the camera center-frame or mobile robot inertial frame in the world coordinates. To turn the generated path into a trajectory, we must append a velocity component for each midpoint. The time values are chosen by spacing proportionally to the distance between two positions of the mobile robot's desired points. Thus, $\Delta t_k = t_k - t_{k-1}$ determine the constant time between two consecutive mobile robot positions in the ground.

3 Kinematic Model

Unsynchronized wheels of mobile robots result in slippage and misalignment in translation and rotation movement [3]. To overcome these problems, the points on the k-th generated trajectories for all wheels have to form a unique instantaneous center of rotation (ICR) (see Fig. 2). Therefore, by knowing the synchronized trajectories midpoints belonging to at least two wheels, we easily obtain ICR point. As illustrated in Fig. 2, generated synchronized trajectories determine the main kinematic variables of mobile robots. The direction of the robot linear velocity vector is determined by the unit vector $\hat{\mathbf{v}}$. Scalar value v is the magnitude of the linear velocity in CP. The angle θ_B is the rotation angle of robot-CP in X direction. θ_B and ψ_v show the angles $\hat{\mathbf{x_0}}$ and $\hat{\mathbf{v}}$ respectively. Variables $\omega_B = \dot{\theta_B}$ and $\omega_v = \dot{\psi_v}$ are the angular velocities of the robot-CP and of $\hat{\mathbf{v}}$ and $\hat{\mathbf{x_0}}$ respectively. The following kinematic constraint describes the relation between robot-CP velocity and the wheels velocities:

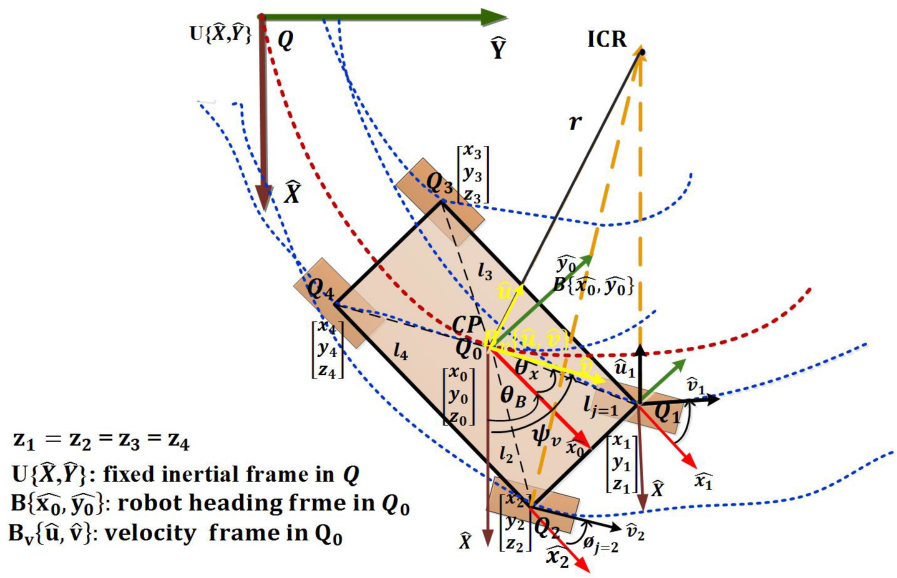

Fig. 2. Generated synchronized trajectories for desired points $\{Q_0, Q_1, ..., Q_4\}$, provide the robot kinematic variables to simplify its kinematic model and estimate ICR using at least two synchronized generated trajectories for instance (Q_1, Q_2).

$$^{\mathbf{B}}\hat{\mathbf{v}} = \mathbf{R}(\psi_v - \theta_B)[1,0,0]^T, \quad v_j^{\mathbf{B}}\hat{\mathbf{v}}_{\mathbf{j}} = v^{\mathbf{B}}\hat{\mathbf{v}} + \omega_B(\hat{\mathbf{z}} \times^{\mathbf{B}} \hat{\ell}_{\mathbf{j}}), \tag{2}$$

where $\mathbf{R}(\psi_v - \theta_B)$ is the rotation matrix with angle $(\psi_v - \theta_B)$ around the $z-$axis, which is frame $\mathbf{B}_v$ in $\mathbf{B}$. $\{^{\mathbf{B}}\hat{\ell}_{\mathbf{j}}, j = 1..4\}$ in frame $\mathbf{B}$ show the constant vectors $\widehat{Q_0 Q_j}$. Angles $\{\phi_j, j = 1..4\}$ are the steering angles of j-th wheel, then $^{\mathbf{B}}\hat{\mathbf{v}}_{\mathbf{j}}$ can be written as $[cos(\phi_j)\ sin(\phi_j)\ 0]$. $v_j^{\mathbf{B}}\hat{\mathbf{v}}_j$ is the velocity vector of $\{Q_j, j = 1..4\}$.

To plan the mobile robot velocities, it is necessary to obtain the mobile robot's ICR with zero velocity while undergoing planar movement in k-th generated trajectories. The relation between ω_B and v_B in the frame $\mathbf{B}$ is:

$$\omega_B = \frac{v_B}{r}, \tag{3}$$

where r is the distance between ICR and CP. v_B and ω_B are the liner and angular velocities of CP respectively. Therefore substituting r in (2) gives the relation between the velocity of the robot-CP and the velocity of its four wheels:

$$v_j = v_B \|\hat{\mathbf{v}} + \frac{1}{r}(\hat{\mathbf{z}} \times \overrightarrow{\ell_{\mathbf{j}}})\|, \{j = 1...4\}. \tag{4}$$

By utilizing the definition of the curvature $\kappa_j = \frac{\dot{\phi}_j}{v_j}$, we can obtain the relation between the driving velocity of each wheel (v_j) and its steering velocity ($\dot{\phi}_j$):

$$\omega_j = \dot{\phi}_j = (\kappa_j.v_B)\|\hat{\mathbf{v}} + \frac{1}{r}(\hat{\mathbf{z}} \times \overrightarrow{\ell_{\mathbf{j}}})\|, \{j = 1...4\}, \tag{5}$$

As illustrated in Fig. 2, the tangent in each point of generated trajectory for each wheel gives $\hat{\mathbf{v}}_{\mathbf{j}}$ and $\hat{\mathbf{u}}_{\mathbf{j}}$. By selecting two generated synchronized trajectories out of four and placing the robot-CP on them, the remaining attached points will coincide with other synchronized generated trajectories. Thus, two v_js are sufficient to calculate the ICR. The distance between the robot-CP and the ICR point r is obtained using the following geometrical relation:

$$r = \sqrt{(x_0 - x_r)^2 + (y_0 - y_r)^2},$$

$$x_r = \frac{v_1.x_2 - v_2(x_1 + v_1(y_1 - y_2))}{v_1 - v_2}, \quad y_r = \frac{x_1 - x_2 + v_1.y_1 - v_2.y_2}{v_1 - v_2}. \tag{6}$$

4 Bounded Velocities Planning

To plan maximum allowable bounded velocities for 4WS mobile robot, we assume maximum driving velocity (V^D_{max}) and maximum steering velocity ($\dot{\phi}^S_{max}$) are known. As explained in Section 3, at each k-th generated trajectories, the curvatures (κ_j), and the relation between v_B and v_j can be calculated. While a mobile robot has four independently steered wheels, there are eight velocity candidates to fulfill four driving and steering constraints. Thus, at each k-th generated trajectories, only one of the driving or steering velocities of each wheel may have maximum value. Therefore, bounded velocities for each wheel are obtained using following steps [4]:

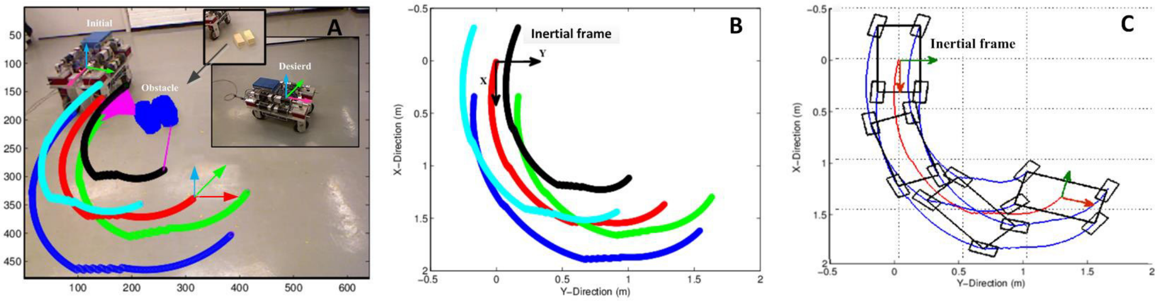

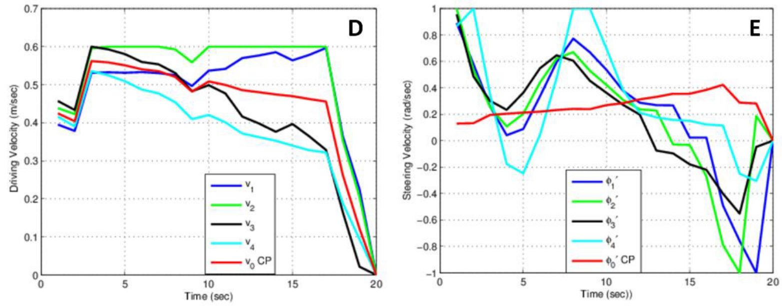

Specifications of the 4WS mobile robot *i*Moro

Description	Quantity
Distance Between Two Wheels (x direction)	655 mm
Distance Between Two Wheels (y direction)	335 mm
Maximum Velocity of Steering Wheel Actuator	$1^{rad}/sec$
Maximum Velocity of Driving Wheel Actuator	$600^{mm}/sec$

Fig. 3. Experiment 1, while *i*Moro must avoid two types of obstacles including recognized static obstacles in the image space (two bricks) and the camera field of view. The generated trajectories between the initial and the desired poses in the image space are illustrated in A, and corresponding trajectories and footprints in the world coordinates are illustrated in B and C respectively. Maximum allowable driving and steering velocities for CP and wheels are illustrated in D and E respectively.

– Evaluate maximum driving velocity of the wheel j ($V_{j,max}$), that keeps its driving and steering velocities bounded:

$$V_{j,max} = min(V^D_{max}, \frac{\dot{\phi}^S_{max}}{\mid \kappa_j \mid}) \tag{7}$$

– Evaluate $v_{B,j}$ as a candidate for the base velocity v_B, that is divided based on the maximum driving velocities of the j wheel:

$$v_{B,j} = \frac{V_{j,max}}{\|(\hat{\mathbf{v}} + \frac{1}{r}(\hat{\mathbf{z}} \times \overrightarrow{\ell_\mathbf{j}})\|} \tag{8}$$

– Evaluate the velocity of CP v_B:

$$v_B = min(v_{B,j}), j \in 1, 2, 3, 4. \tag{9}$$

If κ_j becomes small enough then $V^S_{j,max} = \dot{\phi}^S_{j,max}$ will exceed V^D_{max}. Thus, driving velocity should be bounded by V^D_{max}. If the curvature increases, $V^S_{j,max}$ decreases and steering velocity becomes critical. In this case, driving velocity should not exceed $V^S_{j,max}$. Therefore, steering velocity stays below $\dot{\phi}^S_{max}$.

5 Experiment Results

This section presents the experimental results for 4WS mobile robot called *i*Moro under two different experiments. Our major interest is a mobile robot comprising of a rigid base and four steering wheels, each of which is equipped with two independent servo drives with two DOF in horizontal motion plan. The specification and limits of the wheels actuator velocities of *i*Moro is listed in Fig. 3.

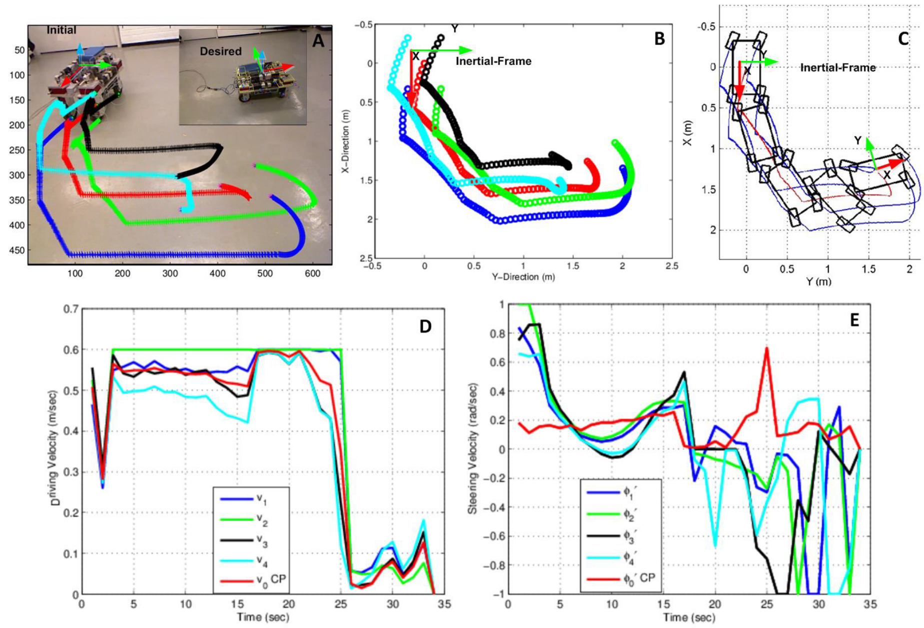

Fig. 4. Experiment 2, while *i*Moro avoids only image boundaries. Generated trajectories in the image space are illustrated in A and corresponding trajectories and footprints in the world coordinates are illustrated in B and C respectively. Planned maximum allowable driving and steering velocities are shown in D and E respectively.

6 Conclusion and Future Work

In this paper, a vision-based trajectory planner (based on an overhead camera) is presented for wheel-steered mobile robots in a confined workspace and in the presence of obstacles. The generated synchronized trajectories simplify the complex kinematic model of mobile robot and plan maximum allowable steering and driving velocities so that at least one of the actuators velocities is at its maximum bound. In the future, this method will be extended to present a vision-based path coordination method for multiple mobile robots in shared and confined workspace to avoid mutual collision.

References

1. Trevelyan, J.P., Kang, S.-C., Hamel, W.R.: Robotics in hazardous applications. In: Springer Handbook of Robotics, pp. 1101–1126. Springer (2008)
2. Ziaei, Z., Oftadeh, R., Mattila, J.: Global path planning with obstacle avoidance for omnidirectional mobile robot using overhead camera. In: 2014 IEEE International Conference on Mechatronics and Automation (ICMA), pp. 697–704. IEEE (2014)
3. Schwesinger, U., Pradalier, C., Siegwart, R.: A novel approach for steering wheel synchronization with velocity/acceleration limits and mechanical constraints. In: 2012 IEEE/RSJ International Conference on Intelligent Robots and Systems (IROS), pp. 5360–5366. IEEE (2012)
4. Oftadeh, R., Aref, M.M., Ghabcheloo, R., Mattila, J.: Bounded-velocity motion control of four wheel steered mobile robots. In: 2013 IEEE/ASME International Conference on Advanced Intelligent Mechatronics (AIM), pp. 255–260. IEEE (2013)

Publication 6

Vision-Based Path Coordination for Multiple Mobile Robots with Four Steering Wheels Using an Overhead Camera

by

Z. Ziaei, R. Oftadeh, and J. Mattila,

Proceeding of the IEEE International Conference On Advanced Intelligent Mechatronics, 2015 (AIM 2015), Busan, Korea,

July 7-11, 2015, pp. 261-268.

Tampereen teknillinen yliopisto
PL 527
33101 Tampere

Tampere University of Technology
P.O.B. 527
FI-33101 Tampere, Finland

ISBN 978-952-15-3717-2
ISSN 1459-2045